Science of the Total Environment 831 (2022) 154902

Contents lists available at ScienceDirect

Science of the Total Environment

journal homepage: www.elsevier.com/locate/scitotenv

Simulation of regional groundwater levels in arid regions using interpretable machine learning models

Qi Liu [a,b], Dongwei Gui [a,*], Lei Zhang [a], Jie Niu [b,**], Heng Dai [c], Guanghui Wei [d], Bill X. Hu [e]

[a] State Key Laboratory of Desert and Oasis Ecology, Xinjiang Institute of Ecology and Geography, Urumqi, Xinjiang, China
[b] College of Life Science and Technology, Jinan University, Guangzhou, Guangdong, China
[c] State Key Laboratory of Biogeology and Environmental Geology, China University of Geosciences, Wuhan, China
[d] Xinjiang Tarim River Basin Management Bureau, Korla, Xinjiang, China
[e] School of Water Conservancy and Environment, University of Jinan, Shandong, China

HIGHLIGHTS

- The machine learning (ML) model is effective in predicting groundwater levels.
- Random Forest performs the best in predicting groundwater levels in this study.
- The shapely additive explanations method is useful for interpreting the ML model.
- No water conveyance for three years will dramatically shrink vegetation area.

GRAPHICAL ABSTRACT

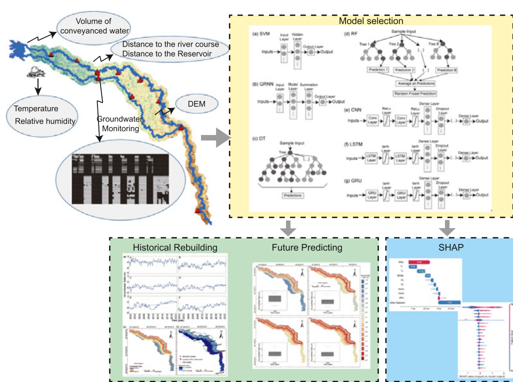

ARTICLE INFO

Article history:
Received 9 January 2022
Received in revised form 24 March 2022
Accepted 25 March 2022
Available online 29 March 2022

Editor: Christian Herrera

Keywords:
Groundwater level
Ecological water conveyance
Arid regions
Machine learning
Deep learning
Shapely additive explanations

ABSTRACT

Regional groundwater level forecasting is critical to water resource management, especially for arid regions which require effective management of groundwater resources to meet human and ecosystem needs. In this study Machine Learning and Deep Learning approaches - Support Vector Machine, Generalized Regression Neural Network, Decision Tree, Random Forest (RF), Convolutional Neural Network, Long Short Term Memory and Gated Recurrent Network- have been used to simulate the groundwater levels in the lower Tarim River basin (LTRB) which is an extreme dryland. The results showed that models developed here with easily available input data such as relative humidity, flow volume and distance to the riverbank can fully utilize spatiotemporally inconsistent groundwater monitoring data to predict the spatiotemporal variation of the groundwater system in arid regions where exist intermittent flow. The shapely additive explanations method was used to interpret the RF model and discover the effect of meteorological, hydrological and environmental variables on the regional groundwater. These explanations showed that the flow volume, the distance to the river channel and reservoir have a critical impact on groundwater changes. Within 300 m distance to the riverbank, groundwater would mainly be influenced by the flow volume and the distance to the reservoir. While far from the riverbank, these effects decreased gradually further away from the river course. The RF prediction results showed that in the next three years (2021 – 2023), the groundwater level on average may decline to −6.4 m, and the suitable areas for natural vegetation growth would be limited to 39% if no water conveyance in the LTRB. To

* Correspondence to: D. Gui, State Key Laboratory of Desert and Oasis Ecology, Xinjiang Institute of Ecology and Geography, Urumqi, Xinjiang, China.
** Correspondence to: J. Niu, College of Life Science and Technology, Jinan University, Guangzhou, Guangdong, China.
E-mail addresses: guidwei@ms.xjb.ac.cn (D. Gui), jniu@jnu.edu.cn (J. Niu).

http://dx.doi.org/10.1016/j.scitotenv.2022.154902

guarantee the stability of ecosystems in the LTRB, it is necessary to convey the water annually. These results can support spatiotemporal predictions of groundwater levels predominantly recharged by intermittent flow, and form a scientific basis for sustainable water resources management in arid regions.

1. Introduction

Groundwater, the world's largest freshwater resource, is an important resource in arid regions. These regions, mostly having average precipitation between 25 and 500 mm year^{-1} (Gaur and Squires, 2018), occupy 41% of global land surface area and are inhabited by roughly more than 2500 million people. Since surface water resources are extremely scarce in these regions, groundwater plays a critical role in the ecological balance, domestic uses, agricultural irrigation, and industrial development (Long et al., 2020). Therefore, an accurate and reliable regional-scale groundwater prediction is critical for the sustainable management of water resources in arid regions. However, groundwater process is a complex nonlinear system dynamically regulated by both natural and anthropogenic factors at different temporal and spatial scales (Wang et al., 2018). Monitoring groundwater levels provides valuable information for understanding system dynamics and detecting long term groundwater behaviors such as replenishment and consumption of groundwater. But in arid regions, groundwater wells are often not adequately distributed spatially across an aquifer because of limitations such as labor and funding (Ruybal et al., 2019). In the meantime, groundwater depth data are usually irregularly collected and have many temporal and spatial gaps in the record. These present challenges in understanding system dynamics and selecting reliable approaches to estimate the spatiotemporal variation of water level fluctuation. In addition, because of climate change, water abstractions, and land use transitions, many previously perennial streams have become intermittent in the past 50 years (Messager et al., 2021). As precipitation is extremely scarce in arid regions, groundwater recharge major occurs through perennial stream, ephemeral stream, and intermittent flow like artificial recharge of water from the river course (Ghayoumian et al., 2007; Hashemi et al., 2013). This intermittent recharge mode further increases the difficulty of regional groundwater simulation in arid regions.

At present, regional groundwater level has been estimated through a variety of techniques, including spatial interpolation models like Kriging Interpolation (Hengl, 2007; Varouchakis and Hristopulos, 2013) and conventional physical-based numerical models such as MODFLOW (Singh, 2014). Although the form of the spatial interpolation models is relatively simple and does not need any physical data, these models are mostly applied for the spatial estimation of groundwater level rather than the temporal one (Tapoglou et al., 2014; Sahoo et al., 2017). Nevertheless, the monitoring wells of arid and semiarid regions are usually sparse and highly non-uniform, which would limit the extensive application of these statistical methods. Physical-based numerical models consider more details of the groundwater processes and provide groundwater fluctuation in the space-time domain (Sherif et al., 2012). But the complexity of real world conditions, such as anisotropy and heterogeneity, cannot be fully expressed. These deficiencies inevitably increase the uncertainty of physics-based model inputs as well as the corresponding output (Szidarovszky et al., 2007). In recent years, the data-driven approaches of Machine Learning (ML) and Deep Learning (DL) are widely used as good alternative approaches compared to conventional models (Wunsch et al., 2018; Yin et al., 2021; Yoon et al., 2011). ML and DL are making major advances in directly solving problems when the physical relations between associated explanatory and explained variables are really difficult to express through conventional process-based models (LeCun et al., 2015). Many studies have shown the usefulness of ML and DL in the temporal prediction of water levels at sampled locations (Tapoglou et al., 2014; Wunsch et al., 2018). To predict groundwater levels in the spatiotemporal domain, various researchers have used ML and DL for temporal prediction and combined with interpolation methods like Kriging Interpolation for spatial estimation (Tapoglou et al., 2014; Sahoo et al., 2017). However, ML and DL have not yet been widely used as a direct approach to predict groundwater levels in the space domain. In fact, ML and DL approaches have already been implemented in other environmental studies in the space-time domain, such as forecasting the spatiotemporal distribution of soil moisture (Fang and Shen, 2020), precipitation (Nguyen et al., 2009), active layer thickness, ground temperature and soil organic carbon (Wang et al., 2020). Hence, it is worth exploring whether ML and DL approaches can be directly used to simulate the spatial and temporal distribution of groundwater levels.

With the development of science and technology, ML and DL have emerged as a collection of advanced models which have been widely implemented for water sciences (LeCun et al., 2015; Shen et al., 2018; Jeihouni et al., 2019). From earlier ML approaches such as Support Vector Machine (SVM), Generalized Regression Neural Network (GRNN), Decision Tree (DT), and Random Forest (RF) to the state of the art DL approaches such as convolutional neural network (CNN), Long Short Term Memory network (LSTM), and Gated Recurrent Units (GRU) neural network, there are various models that have shown the possibility to estimate groundwater levels (Dilip and Rajib, 2021; Koch et al., 2019; Rajaee et al., 2019). All types of ML and DL models have advantages and disadvantages, and it is challenging to select the appropriate models that simulate water levels with high accuracy. Furthermore, many water scientists are reluctant to use ML and DL because they are "black boxes" that we cannot understand how the model uses input variables to make predictions (Wang et al., 2022). Recently, Shapely additive explanation (SHAP) has been successfully adopted in the interpretation of ML and DL (Lundberg and Lee, 2017). SHAP can exhibit the effect of each input variable on the model output from the local and global perspective, and it has been successfully applied in many fields (Wang et al., 2021, 2022; Yang et al., 2021).

In this study, the lower Tarim River basin is considered the study site. Tarim River basin is the largest inland river basin in China and has a dry, desert climate (Tao et al., 2008). The groundwater level in the mainstream is mainly recharged by the stream and the survival of natural vegetation along the lower reaches depends almost entirely on groundwater (Hao et al., 2010). In the lower reaches of the Tarim River, streamflow has completely dried up since 1970 due to large scale anthropogenic activities such as irrigation. To revive the degraded ecosystem of the lower Tarim River, the Chinese Government started to implement the "Ecological Water Conveyance" project by intermittently transporting freshwater from the upper reaches through the river channel to the lower reaches (Tao et al., 2008). To facilitate management of water resources, an accurate simulation of groundwater level in the lower Tarim River basin is needed.

The objective of this study is to develop a model to predict the spatiotemporal distribution of groundwater levels in arid regions where groundwater recharge major occurs through runoff or intermittent flow like artificial recharge of water from the river course, and quantitatively estimate the present and future status of groundwater in the lower Tarim River basin. The model developed here is intended to fully utilize spatiotemporally inconsistent groundwater monitoring data to reconstruct the spatiotemporal variation of the groundwater system in arid regions where exist stream or intermittent flow. Furthermore, the SHAP method can provide a novel perspective to quantify the relationships between groundwater variation and meteorological, hydrological and environmental factors. Specifically, this work has four objectives: 1) To compare the predictive ability on regional groundwater levels in the lower Tarim River basin of the four popular ML models (SVM, GRNN, DT, and RF) and three DL models (CNN, LSTM, and GRU) and determine the optimum modeling based on statistical performance metrics; 2) to use SHAP to interpret the optimum modeling and understand how each input variable affects the regional groundwater level; 3) to use optimal modeling to simulate the present groundwater forced by the "Ecological Water Conveyance" project and detect the interannual variation of groundwater level downstream of Tarim River; 4) to apply the optimal model to predict future groundwater tables in the next three years. The prediction of regional groundwater levels can provide useful information for the study of ecology and hydrology resulting from groundwater level change on the lower Tarim River basin, and serve as a reference to arid regions where groundwater recharge major occurs through runoff or intermittent flow like artificial recharge of water from the river course.

2. Materials and methods

2.1. Study site and data sources

The Tarim River basin with an area of approximately 1.02×10^6 km^2, which is located near the Taklimakan Desert, is one of the largest closed hydrological drainage systems in the world (Fig. 1(a)). In hydrological terms, the Tarim River was fed by precipitation at middle mountains and glacier melt and snowmelt water from high mountainous areas (Yang et al., 2019). Because of climate change and intensive water exploitation, many headstreams have lost surface hydraulic links with the mainstream of the Tarim River basin. At present, only the Aksu, Yarkant, and Hotan Rivers supply water to the Tarim River basin (Fig. 1(a)). The climate of the Tarim River basin is characterized by an extremely arid, desert climate with an annual rainfall below 35 mm, temperatures ranging from −35 °C to 40 °C, annual sunshine duration of 2800–3100 h, and annual potential evaporation of approximately 2590 mm (Huang and Pang, 2010). The annual potential evaporation data were calculated using the Penman-Monteith method (Allen et al., 1998) based on climate data obtained through the meteorological stations in the Tarim River basin. The vegetation of this region is sparse and largely follows the riverbank to form green belts. The vegetation types in the region mainly include herbs like *Poacynum hendersonii*, *Phragmites communis*, *Glyzyrrhiza inflate*, *Alhagi sparsifolia*, and *Karelinia caspica*, arbors like *Populus euphratica*, and shrubs like *Tamarix* spp., *Halimodendron halodendron*, *Lycium ruthenicum*, and *Nitraria sibirica* (Hao et al., 2010). Since the precipitation in the area cannot

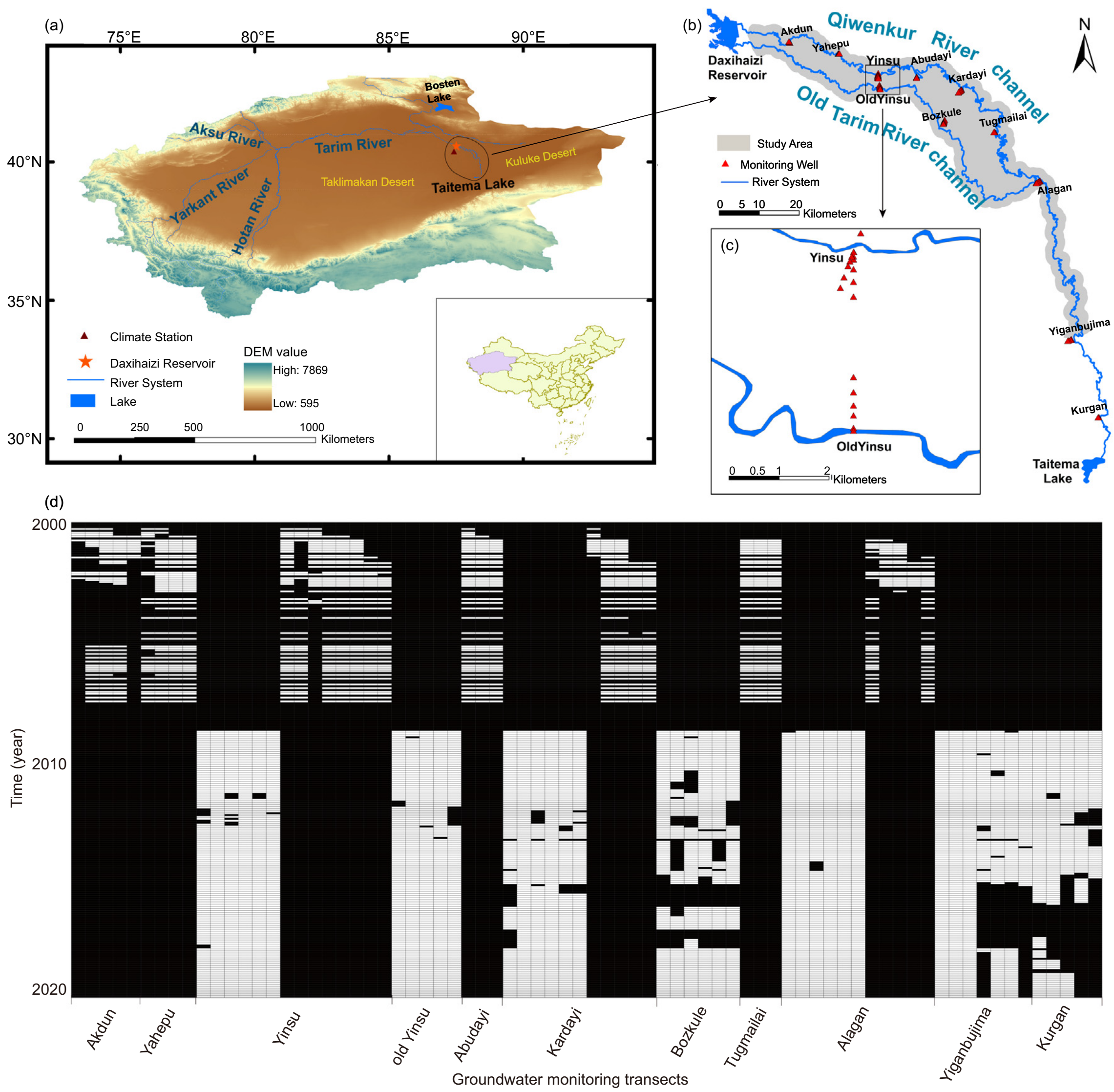

Fig. 1. (a) Study area of Tarim River basin, with (b) marked locations of the 74 groundwater monitoring wells for in-situ observations of the groundwater table. (c) illustrates the region of two river courses between Yinsu and Old Yinsu, an enlargement of a portion of (b). The gray area denotes the study area. (d) The grid diagram illustrates the available monthly groundwater level data for 74 groundwater monitoring wells in the lower Tarim River basin from January 2000 to December 2020. Each column represents a unique groundwater monitoring well while each row denotes a month. The black square denotes the missing value while the gray square denotes the available value. Groundwater wells are arranged from decreasing latitude (top to bottom) and highlight the irregularity of groundwater table monitoring and temporal sparseness of the monitoring data.

meet the requirement of natural vegetation, the survival of the vegetation communities mainly depends on the groundwater while the groundwater is mainly recharged by stream (Tao et al., 2008).

In this work, the study focuses on the downstream of Tarim River basin, which is stretched from Daxihaizi Reservoir to Taitema Lake (Fig. 1(b)). The lower reaches of the Tarim River is known as the 'Green Corridor' since it is located between the Taklimakan Desert and the Kuluke Desert and protects the railroad along the river (Tao et al., 2008). Since the 1960s, changing climate, and intensive anthropogenic activities in the upper and middle reaches of the Tarim River have significantly reduced the stream flow into the lower reaches. Moreover, after the construction of the Daxihaizi Reservoir in 1972, the downstream streamflow has been completely dried up (Song et al., 1999). Consequently, having no streamflow in the lower reaches, Taitema Lake became dried up, groundwater tables dropped sharply, the basin's downstream ecosystems were seriously degraded, and desertification and salinization expanded rapidly. To save the 'Green Corridor', the Central Chinese Government started to "Ecological Water Conveyance" project since 2000, that is from the upper Tarim River and neighboring Bosten Lake to the lower reaches (Ling et al., 2016). The project generally transported water from the Daxihaizi Reservoir, and then to the lower reaches through the single river canal or double river canal (i.e., either the Qiwenkur river channel or the Old Tarim river channel, or both) (Fig. 1(b)). As a result of this project, groundwater tables have increased significantly and degraded ecosystems have been effectively restored in the lower reaches of the Tarim River (Mamat et al., 2018).

Eleven groundwater monitoring transects, 50 m wide and 450–1500 m long (including a total of 74 groundwater monitoring wells) were established along the river course to observe groundwater levels (Fig. 1(b)). They are located in the transects of Akdun, Yahepu, Yinsu, old Yinsu, Abudayi, Kardayi, Bozkule, Tugmailai, Alagan, Yiganbujima, and Kurgan downstream of the Daxihaizi Reservoir. For each transect, six or five groundwater monitoring wells were installed at distances of 50, 150, 300, 500, 750, and 1050 m from the riverway in the lower reaches (Fig. 1 (b) and (c)). Groundwater level data were obtained every month during the period from 2000 to 2020. Fig. 1(d) illustrates the available monthly groundwater monitoring data for 74 groundwater monitoring wells in the lower reaches from January 2000 to December 2020. Each column represents a groundwater monitoring well while each row denotes a month. Groundwater monitoring wells are arranged from decreasing latitude (top to bottom). To highlight the irregularity of groundwater table monitoring and temporal sparseness of the monitoring data, the gray square denotes the available groundwater table data while the black square denotes the missing value as some wells were damaged. There were significant spatio-temporal gaps for the records of groundwater level observations. Some well records only include periods between 2000 and 2007 whereas others only included observations between 2009 and 2020 (Fig. 1(d)). Because of limitations such as labor and funding in arid and semiarid regions, monitoring wells in these regions often lack regular maintenance and rehabilitation (Ruybal et al., 2019). None of the wells had a continuous observation record between 2000 and 2020, while fewer than 17% of the well records included a continuous observation of the months between 2009 and 2020 (Fig. 1(d)). This is a generic problem that is prevalent in many arid and semiarid areas, and will significantly increase the difficulty of groundwater simulation (Ruybal et al., 2019).

In order to retain the physical meaning of the network, all input parameters are directly or indirectly related to the water balance equation. Among the input parameters, more specifically, the temperature and relative humidity are related to evapotranspiration (Wunsch et al., 2021; Yin et al., 2021) while the "Ecological Water Conveyance" project is directly related to the groundwater recharge. The precipitation is ignored here since it is too little to contribute to groundwater supply in arid and semiarid regions (Hao et al., 2010). Because the groundwater levels have a memory with respect to previous climate and human activities over timescales of less than one year (Russo and Lall, 2017), input parameters of 6 previous months are considered here. Moreover, groundwater configuration is also controlled by the topography, and is usually a replication of the topography (Condon and Maxwell, 2015). The digital elevation model (DEM) with a resolution of 30 m (available at http://www.tpedatabase.cn/), and the distances to the adjacent river channel and to the Daxihaizi Reservoir, which are taken as surrogates for the topography, are also selected as model inputs since they directly affect the extent of groundwater recharge. In summary, the hydraulic head change in the current month (t) is predicted through temperature, relative humidity, and the volume of water conveyanced from the river course in the current month (t) and 6 previous months (t-6, t-5, t-4, t-3, t-2, t-1), and geospatial information (DEM, distances to the nearest river channel and to the Daxihaizi Reservoir). In order to have a complete picture of all the variables acting on the modeling, all the input variables are listed in Table 1, which account for the effects of meteorological, hydrological, and environmental factors. In general, these input parameters are easy to measure and widely available. This makes this approach, in principle, easily transferable and hence applicable to other arid regions where groundwater is mainly recharged by the stream or intermittent flow through the river course.

The monthly air temperature and relative humidity data between 1999 and 2020 were collected from climatological station. The monthly volume of water conveyanced from the Daxihaizi Reservoir to the Qiwenkur River channel and Old Tarim River channel were obtained from the Tarim River Basin Administration. To predict the spatiotemporal changes of downstream groundwater levels of the Tarim River basin during 2021–2023, temperature and relative humidity data over the study area were derived from four climate models (i.e., CanESM5, INM-CM5-0, IPSL-CM6A-LR, and MRI-ESM2-0) of the coupled model intercomparison project phase 6 (CMIP6) under scenario SSP245 (shared socioeconomic pathway representative concentration pathway, SSP) (O'Neill et al., 2016). The climate model outputs have been bias-corrected against climate station data.

2.2. Model description and implementation

2.2.1. Model description

In this study, four ML models and three DL models were selected to fit the groundwater level in the lower Tarim River. The four ML models are Support Vector Machine (SVM), Generalized Regression Neural Network (GRNN), Decision Tree (DT) and Random Forest (RF). And the three DL models are convolutional neural network (CNN), Long Short Term Memory network (LSTM), and Gated Recurrent Units (GRU) neural network. All the models are summarized in Table 2. SVM regression is considered a non-parametric approach since it relies on kernel functions (Smola, 1998). GRNN is a variant of the radial basis network (Specht, 1991), has only one adjustable parameter is easy to tune and has less training time. DT is regarded as the most easily understandable ML approach (Breiman et al., 1984), but has the risk of overfitting as it tends to fit all the samples within the training data closely. RF creates a forest by combining the predictions of multiple DT models, and can effectively avoid overfitting since the averaging of uncorrelated trees reduces the overall variance and prediction error

Table 1
List of model inputs in the model.

Indicator group	Metric code	Metric description
Meteorological indicators	$temp_t$	Monthly temperature (°C) lead t month, t = 0,1, …,6
	hum_t	Monthly relative humidity (%) lead t month, t = 0,1, …,6
Hydrological indicators	$Q_{D\text{-}t}$	Monthly total volume of conveyanced water in Daxihaizi Reservoir lead t month (10^8 m^3), t = 0,1, …,6
	$Q_{O\text{-}t}$	Monthly total volume of conveyanced water in old Tarim river channel lead t month (10^8 m^3), t = 0,1, …,6
	$Q_{Q\text{-}t}$	Monthly total volume of conveyanced water in Qiwenkur river channel lead t month (10^8 m^3), t = 0,1, …,6
Environmental descriptors	DEM	Altitude (m)
	$dist_D$	Distance to the Daxihaizi Reservoir (m)
	$dist_O$	Distance to the nearest Old Tarim River channel (m)
	$dist_Q$	Distance to the nearest Qiwenkur River channel (m)
	$dist_L$	Distance to the nearest lower section of lower Tarim River channel (m)

Table 2
Summary of the support vector machine (SVM), generalized regression neural network (GRNN), decision tree (DT), random forest (RF), convolutional neural network (CNN), long short term memory network (LSTM), and gated recurrent units (GRU) neural network.

Category	Approach	Description	Strength	Weakness
Machine learning	SVM	Mapping the nonlinear dataset to higher dimensional feature space through different types of kernel functions.	Less training time.	Not suitable for large data sets.
	GRNN	A variant of the radial basis network, can deal with linear and nonlinear data.	Easy to tune.	Easy to overfit.
	DT	Modeling the data as a tree of hierarchical branches and uses a group of binary rules to calculate the target value.	Easy to explain.	Easy to overfit.
	RF	A collection of DT models that combines the predictions of the DT models to produce a more accurate prediction.	Not easy to overfit	Slower.
Deep learning	CNN	Contains one or more convolutional layers that can be either entirely connected or pooled.	Works well in feature extraction.	Large training data needed; hardware dependence; slower.
	LSTM	A kind of the recurrent neural network, which avoids the vanishing gradient problem by gated regulators.	Works well in time series prediction.	
	GRU	A variant of the LSTM model and does not contain separate memory cells.	Faster and simpler than LSTM.	

(Breiman, 2001). CNN is a DL method that is particularly used for image and audio processing (LeCun et al., 2015). Li et al. (2018) proposed a new one-dimensional time series prediction algorithm through two-dimensional CNNs and is more appropriate for the feature extraction from multiple one-dimensional time series. LSTM is a kind of recurrent neural network that is widely used to model time series in the field of DL, can effectively avoid vanishing and exploding gradient issues (Fang and Shen, 2020). Similar to LSTM, GRU is also a kind of recurrent neural network but is simpler and faster than LSTM and often offers comparable performance to that of LSTM (Chung et al., 2014).

2.2.2. Model training and evaluation

In this study, all the models are trained using a random sample of 75% of the observation data and tested using the remaining 25% data. In addition, to converge faster and prevent local extremes from affecting training, the input variables are normalized to the range of −1 to 1 before training. Hyperparameters for each model are tuned manually. In addition, each DL model (i.e., CNN, LSTM, and GRU) is trained for 120 epochs with a mini-batch size of 512 and data shuffled every epoch to make the neural network robust. The Adam algorithm with an initial learning rate of 0.005 and a dropping factor of 0.2 is employed. Gradient clipping is applied to prevent gradient explosion. Early stopping is used to prevent overfitting and to improve the ability of model generalization. The calculations of these models are performed on the CPU (Intel(R) Core(TM) i5-10210U CPU @ 1.60 GHz).

Model performances are assessed for the test data through the following metrics: squared Pearson's correlation coefficient (R^2), root mean squared error (*RMSE*), percentual bias (*PBIAS*), and mean absolute relative error (*MARE*):

$$\mathrm{R}^2 = \left(\frac{\sum_{i=1}^{n}(o_i-\overline{o})(p_i-\overline{p})}{\sqrt{\sum_{i=1}^{n}(o_i-\overline{o})^2}\sqrt{\sum_{i=1}^{n}(p_i-\overline{p})^2}}\right)^2 \tag{1}$$

$$\mathrm{RMSE} = \sqrt{\frac{1}{n}\sum_{i=1}^{n}(p_i-o_i)^2} \tag{2}$$

$$\mathrm{PBIAS} = 100\frac{\sum_{i=1}^{n}(p_i-o_i)}{\sum_{i=1}^{n}(o_i)} \tag{3}$$

$$\mathrm{MARE} = \frac{1}{n}\sum_{i=1}^{n}\left|\frac{p_i-o_i}{o_{\max}-o_{\min}}\right| \tag{4}$$

where o_i and p_i denote the observed and predicted groundwater levels, respectively. i refers to the ith value of the data. n is the number of observations. $\overline{o}$ is the mean observation. $o_{\max}$ and $o_{\min}$ represent the maximum and minimum values of observation, respectively. R^2 is a general determination coefficient, which compares the linear correlation between predictions and observations. RMSE is the standard deviation of the prediction errors and is penalized by large errors since its errors are squared. The PBIAS is the average prediction errors concerning the average of the observed data, and it shows whether the model tends to underestimate or overestimate the observations (Gupta et al., 1999). The MARE indicates the average magnitude of the relative error between simulated and observed data. The ideal scores for the goodness-of-fit criteria are 1 for R^2, and 0 for RMSE, PBIAS, and MARE. Model performance is assessed using a repeated loop of 100.

2.3. SHAP

SHAP method is a game theoretic approach that can interpret ML models (Lundberg and Lee, 2017). Unlike conventional methods that can only exhibit the degree of influence of input variables on the model output, SHAP can also show the positive or negative effect of each variable on the model (Wang et al., 2022). With a trained ML model M, and input variables $x = \{x_1, \cdots, x_q\}$, SHAP can use an explanation model E to determine the contribution of each variable to model M. The details of SHAP are described in the following equations:

$$\mathrm{E} = \phi_0 + \sum_{i=1}^{q}\phi_i t_i \tag{5}$$

where q is the number of input variables, t is the simplification of the variable, and $\phi_i \in R$ denotes the contribution of each variable to the ML model (Wang et al., 2022). The function ϕ can be described as:

$$\phi_i(\mathrm{M}, \mathrm{x}) = \sum_{t\subseteq x}\frac{|t|!(q-|t|-1)!}{q!}\left[\mathrm{M}(t)-\mathrm{M}(t\backslash i)\right] \tag{6}$$

where \ is the difference-set notation for set operations. The SHAP results were derived using the “shap” package in Python 3.0.

2.4. Trend analysis

Theil-Sen's slope is a nonparametric approach to estimate the slope of trend and requires no assumption on the probability distribution of the dataset (Sen, 1968). The slope *S* of time series x_1, ..., x_n is given by

$$\mathrm{S} = \mathrm{Median}\left(\frac{x_j - x_i}{j-i}\right) \quad \text{for all } i < j \tag{7}$$

where $1 < i < j < n$. A positive *S* denotes an increasing trend, and a negative *S* denotes a decreasing trend.

3. Results and discussion

3.1. Performance assessment for different models

To fully investigate the model performance, the average performances from all seven models (i.e., SVM, GRNN, DT, RF, CNN, LSTM, and GRU, each with 100 well-trained models) are summarized and compared in Fig. 2. Fig. 2 shows that on average, RF models perform the best with a higher R^2 value of 0.87 on average, followed by DT, GRU, LSTM, and CNN models. In contrast, SVM and GRNN models exhibit the least accurate results. This is consistent for all metrics except PBIAS, where SVM and GRNN models show slightly less bias than GRU, LSTM, and CNN models (Fig. 2). Additionally, Fig. 2(e) shows the calculation speed of these model types. As expected, ML methods (i.e., SVM, GRNN, DT, and RF) in general are less expensive than DL methods (i.e., CNN, LSTM, and GRU). For example, the associated time needed for the LSTM model is 13 folds of the time used for the RF model. Because compared with ML approaches, the learning process of DL models is deep as the structure of DL modeling has multiple hidden layers (LeCun et al., 2015). Consistent with previous studies (Chung et al., 2014), LSTM and GRU networks present almost equal performance since they are based on the recurrent neural network, and the computation speed of GRU is faster than that of LSTM due to its simplicity (Fig. 2(b)).

The general superiority of RF over other ML methods such as DT, SVM, and GRNN in the prediction of groundwater level is expected because it is an ensemble-based approach and often performs better than other ML methods in previous studies (Shen et al., 2018; Yin et al., 2021). However, RF and DT approaches here are also superior to DL approaches in predicting groundwater levels. Theoretically, DL approaches, especially the LSTM and GRU networks, are known as accurate time series predicting models because of their memory cell structures that allow them to remember information over a long period (Wunsch et al., 2021). DL methods may perform better in multistep-ahead forecasting as they are designed to process long sequence data. However, a one-step-ahead forecast instead of a multistep-ahead forecast is considered here because the record of groundwater monitoring data has many gaps in time and space horizons (Fig. 1d). In addition, the mediocre performance of DL methods may also relate to the size of samples used in this study, which is not large enough to support the establishment of complex DL methods, and resulting in the underutilization of the ability of DL methods (Shen et al., 2018). In this study, DL methods still show superiority over some ML methods such as SVM and GRMM because SVM and GRNN are not effective for time series prediction as they are not

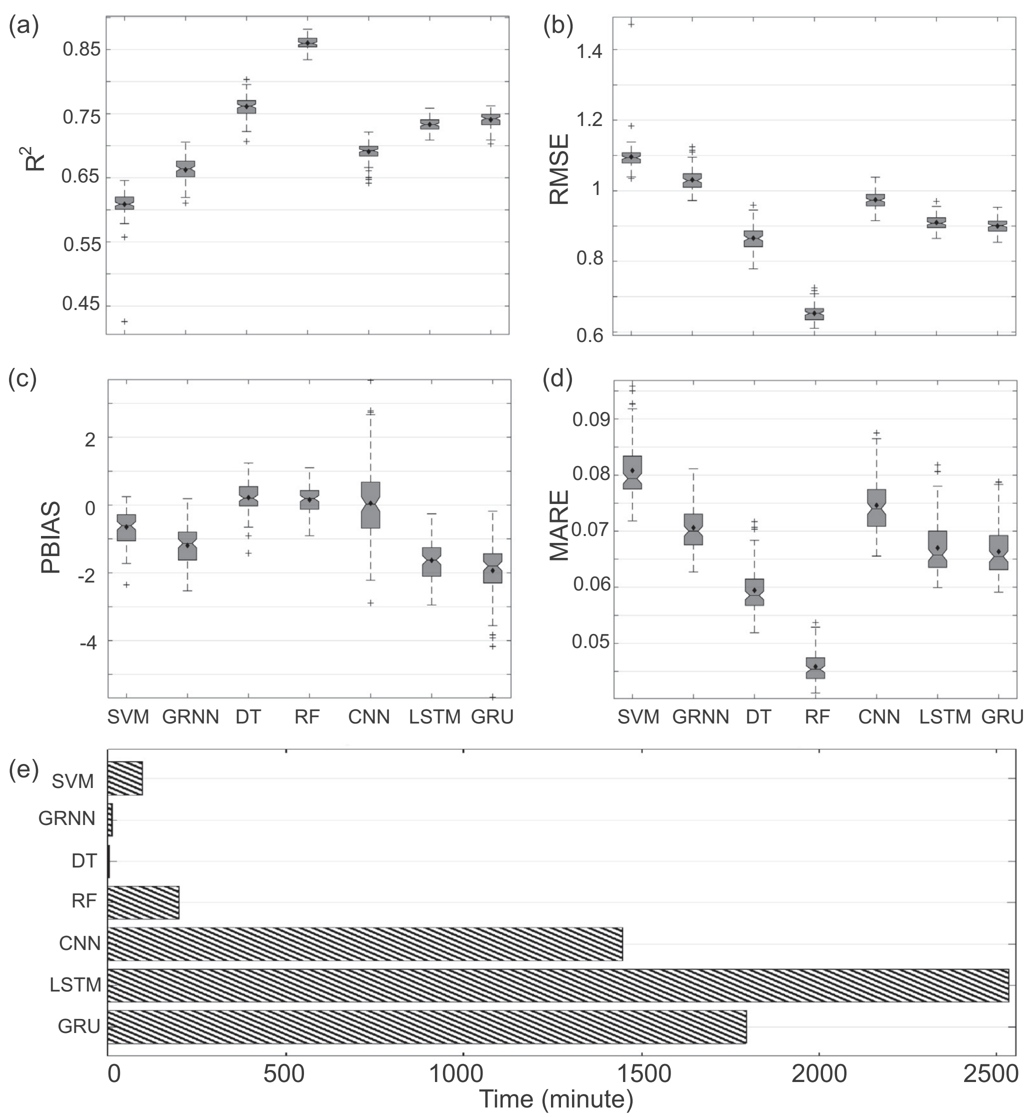

Fig. 2. (a–d) Boxplots showing the prediction accuracy of well-trained SVM, GRNN, DT, RF, CNN, LSTM, and GRU models (each with 100 model runs) for the test dataset. The diamond symbols indicate the arithmetic mean. (e) Barplot showing the total time spent on training SVM, GRNN, DT, RF, CNN, LSTM, and GRU models 100 times.

suitable for large sample feature scale and sensitive to outliers (Gaye et al., 2021; Montano et al., 2011). GRNN tends to show poor generalization ability for highly correlated data (Montano et al., 2011). These results also indicate that the model should be selected carefully although ML and DL models can capture the groundwater variations in arid regions, there still exists some divergence in the performance of different model types.

ML/DL approaches were initially used as alternatives to process-based models in the prediction of groundwater levels due to their high accuracy with less time and cost (Yin et al., 2021; Wunsch et al., 2018; Yoon et al., 2011). Many studies also have compared the performance of groundwater level prediction between the ML/DL approaches and process-based models, and most of them found that ML/DL models can provide more accurate predictions than physically-based models (Zeydalinejad, 2022; Chen et al., 2020; Moghaddam et al., 2019). However, physically-based models possess simplified expressions of the underlying physical mechanism of the groundwater system, while data-driven ML/DL approaches contain no such information explicitly. And it suggests potential in hybrid physics-ML approaches that can combine hydrological mechanisms with high prediction accuracy. Therefore, some studies recently have integrated ML with physics-based models to develop physics informed neural networks, which contain the law of physics described by the physics-based models (Chen et al., 2021; Raissi et al., 2017, 2018). Besides, ML/DL models also were used to learn a global mapping between raw inputs and parameters of the process-based model, which are then fed into the differentiable process-based model, and can be a surrogate of traditional parameter calibration (Tsai et al., 2021). In summary, with the development of artificial intelligence, the relation between ML/DL models and process-based models has now changed from solely competitive to integrative and cooperative. However, the ML models used in this study were merely a data-driven surrogate to a process-based model. Further research should attempt to develop a new hybrid physics-ML model that injects the physical mechanism of groundwater dynamics into ML algorithms and thereby make it more understandable.

3.2. Model interpretation

Because the RF model performs best in simulating groundwater levels, the SHAP method was used to interpret the RF model. The overall importance of each input variable (Table 3) was calculated as the average of the absolute SHAP values for each input variable. A greater mean SHAP value corresponds to a greater influence on the model output (Wang et al., 2022). Table 3 shows that the variables $dist_Q$, $dist_O$, $Q_{D\text{-}1}$, $Q_{O\text{-}6}$, $Q_{Q\text{-}6}$ and $dist_D$ (see Table 1 for the explanation of the acronyms) all have a large impact on the groundwater level.

The SHAP summary plot (Fig. 3) was used to further see the magnitude and direction of the effect of a variable (Lundberg and Lee, 2017). We present the twenty most important features and visualize their associations with groundwater level. It is obvious from Fig. 3 that the volume of conveyanced water with a lead of 0–6 months, $dist_Q$, and $dist_O$ are the variables that most affect groundwater level in the lower reaches of the Tarim River. Where an increase in the volume of conveyanced water, especially of $Q_{O\text{-}6}$, $Q_{D\text{-}1}$, $Q_{D\text{-}6}$, and $Q_{Q\text{-}6}$, correspond to an increase in SHAP value and shows a potentially positive impact on groundwater level (Fig. 3). A closer distance to the river course has a higher SHAP value, with a larger positive impact on groundwater levels (Fig. 3). Environmental factors like $dist_D$ and DEM are the next most critical factors while the effect of meteorological factors on the change of groundwater depth in the lower Tarim River is small. Large values of $dist_D$ and DEM correspond to negative SHAP values and show negative correlations with groundwater level (Fig. 3).

SHAP interaction plots (Fig. 4) show how the effect of a variable on model output varies with other variables (Lundberg and Lee, 2017). We present the SHAP interaction values between the important variables $dist_Q$, $Q_{D\text{-}1}$, $dist_D$, and DEM, and visualize their interaction effects on groundwater level. The interaction effects of $dist_Q$ with variables $Q_{D\text{-}1}$, $dist_D$, and DEM (Fig. 4a – f) show how the effect of $dist_Q$ on groundwater depth varies with them. Within 300 m distance to the river course (i.e., $dist_Q < 300$ m), conveyanced more water (i.e., $Q_{D\text{-}1} > 0.7 \times 10^8$ m^3) and the nearest distance to Daxihaizi Reservoir (i.e., $dist_D < 45$ km) can dramatically lifts the groundwater level (Fig. 4b–c). While far from the river channel (i.e., $dist_Q > 300$ m), lower altitude can lift the groundwater level (i.e., DEM < 820 m; Fig. 4d), and the effects of variables $Q_{D\text{-}1}$, $dist_D$ on groundwater depth decreased gradually further away from the river course (Fig. 4b–c). Similarly, the interaction effects within $Q_{D\text{-}1}$, $dist_D$, and DEM (Fig. 4e–j) show consistent results that compared with places far from the Daxihaizi Reservoir and higher altitude, having the nearest distance to the Daxihaizi Reservoir and lower altitude can lift the groundwater level. These results (Figs. 3 and 4) agree with existing literature (Tao et al., 2008; Chen et al., 2010; Liu et al., 2019) that the water conveyance project in the lower Tarim River basin plays an important role in lifting the groundwater level close to the river channel, and the response of groundwater level decreased gradually further down the river course and decreased gradually further away from the river course. This might be because the rainfall in the lower Tarim River basin is scarce, and conveyanced water is the dominant recharge source of groundwater (Tao et al., 2008).

Table 3
variable importance for the prediction of groundwater in the lower Tarim River basin.

Old Tarim river channel		Qiwenkur river channel		Lower section of lower Tarim River		Overall model	
Variable	Importance	Variable	Importance	Variable	Importance	Variable	Importance
$dist_Q$	1.03	$dist_Q$	0.92	$dist_Q$	0.75	$dist_Q$	0.89
$Q_{O\text{-}6}$	0.27	$Q_{D\text{-}1}$	0.18	$Q_{O\text{-}6}$	0.23	$Q_{O\text{-}6}$	0.21
$Q_{D\text{-}1}$	0.19	$dist_O$	0.17	$dist_D$	0.17	$Q_{D\text{-}1}$	0.18
$dist_O$	0.12	$Q_{Q\text{-}6}$	0.17	$Q_{D\text{-}1}$	0.16	$dist_O$	0.18
$Q_{D\text{-}6}$	0.11	$Q_{D\text{-}6}$	0.12	$dist_O$	0.11	$dist_D$	0.11
$Q_{D\text{-}3}$	0.1	$dist_D$	0.11	$Q_{D\text{-}6}$	0.09	$Q_{D\text{-}6}$	0.1
$Q_{D\text{-}0}$	0.09	$Q_{D\text{-}3}$	0.06	$Q_{D\text{-}3}$	0.08	$Q_{D\text{-}3}$	0.08
$dist_D$	0.07	DEM	0.06	$Q_{D\text{-}0}$	0.06	$Q_{D\text{-}0}$	0.06
$Q_{O\text{-}5}$	0.07	$Q_{Q\text{-}1}$	0.05	$Q_{O\text{-}5}$	0.06	$Q_{O\text{-}5}$	0.06
$Q_{O\text{-}3}$	0.06	$Q_{O\text{-}5}$	0.05	$Q_{D\text{-}2}$	0.05	DEM	0.06
hum_2	0.05	$Q_{D\text{-}0}$	0.05	DEM	0.05	$Q_{D\text{-}2}$	0.05
hum_3	0.05	$Q_{D\text{-}2}$	0.04	hum_3	0.05	$Q_{O\text{-}3}$	0.04
$Q_{D\text{-}2}$	0.05	$Q_{O\text{-}2}$	0.03	hum_2	0.05	hum_2	0.04
$Q_{O\text{-}0}$	0.04	$Q_{O\text{-}3}$	0.03	$Q_{D\text{-}4}$	0.04	hum_3	0.04
hum_6	0.04	hum_2	0.03	hum_6	0.04	hum_6	0.03
$Q_{D\text{-}4}$	0.03	hum_3	0.03	$Q_{O\text{-}2}$	0.04	$Q_{D\text{-}4}$	0.03
$Q_{O\text{-}2}$	0.03	$Q_{D\text{-}4}$	0.03	$Q_{O\text{-}3}$	0.04	$Q_{O\text{-}2}$	0.03
$Q_{Q\text{-}1}$	0.03	$temp_4$	0.03	hum_5	0.03	$Q_{Q\text{-}1}$	0.03
hum_4	0.03	$Q_{Q\text{-}0}$	0.02	hum_4	0.03	hum_4	0.03
$Q_{Q\text{-}6}$	0.03	$Q_{O\text{-}6}$	0.02	$Q_{Q\text{-}6}$	0.03	$Q_{Q\text{-}6}$	0.03

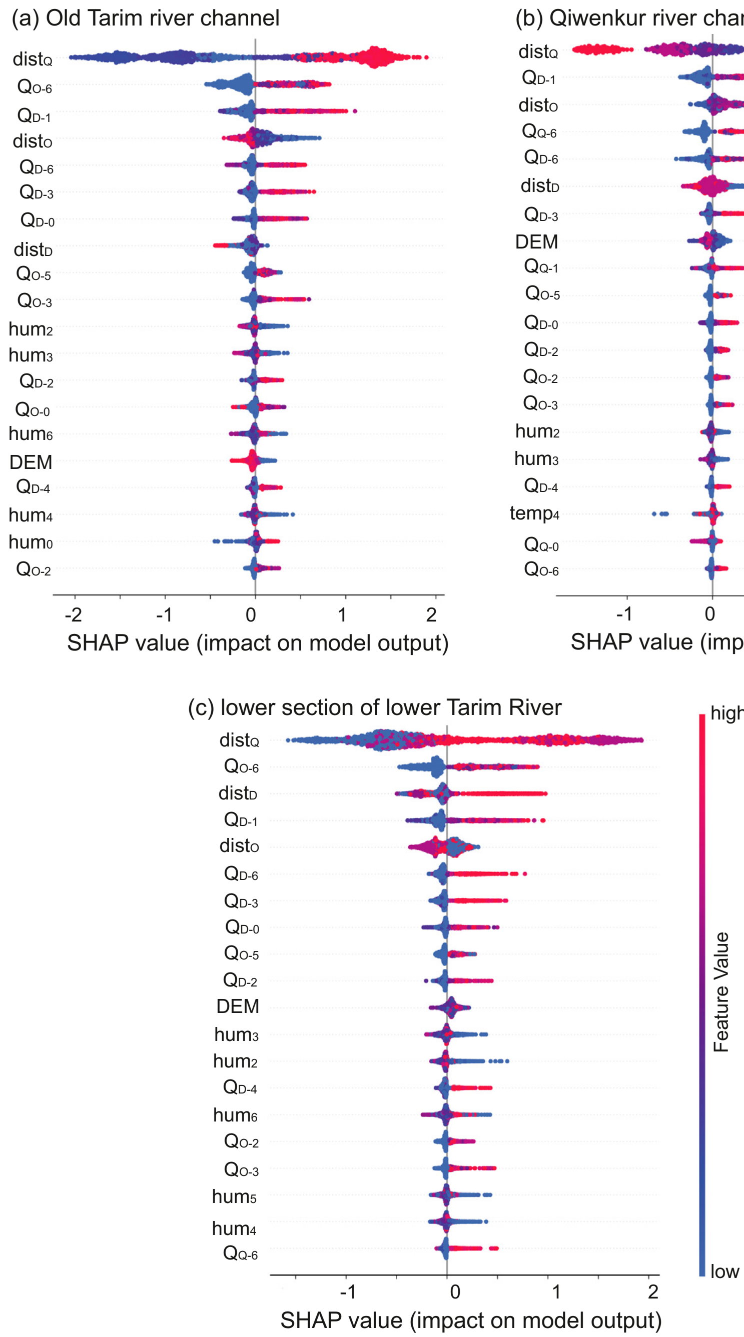

Fig. 3. SHAP summary results of feature importance from the RF model in (a) the Old Tarim river channel, (b) the Qiwenkur river channel, and (c) the lower section of the lower Tarim River basin. The vertical axis lists the model input, and the horizontal axis exhibits the impact that variable has on the model's prediction for groundwater level. The red color denotes a higher value of variables while the blue denotes a lower value. For the metric codes of the variables see Table 1.

Furthermore, the variable DEM shows a negative impact on groundwater level while an increase in DEM also implies a drop in the groundwater level. This result is consistent with previous analysis (Condon and Maxwell, 2015) that, on a regional scale, the groundwater level is connected to the topography, and is usually a subdued version of topography.

Because traditional process-based models such as MODFLOW, HYDRUS can efficiently reproduce the physical process of groundwater dynamic, they are widely used to explore the mechanism of a groundwater system (Sherif et al., 2012). However, there are still many deficiencies in the implementation of process-based models to groundwater prediction, and they are plagued by issues of complexity and nonlinearity of physical processes, uncertainty in parameterization processes, and contradictions in spatial and temporal scales (Basu et al., 2022; Govindaraju, 2000). In recent years, as data-driven models like ML and DL methods can obtain robust results with less time and cost in various complex groundwater systems, many researchers have gradually adopted them for groundwater prediction (Sahoo et al., 2017; Wunsch et al., 2018; Yoon et al., 2011). Nevertheless, the deficiency of these data-driven models is that they are of the "black box" type and do not provide any explicit expression to quantify the effect of each variable on the model output (Basu et al., 2022). Therefore, many scientists are reluctant to adopt ML and DL models in the field of water environment sciences (Nearing et al., 2020). To overcome this constraint, the SHAP method (Lundberg and Lee, 2017), which studies how the model uses variables to make predictions, can compensate for the ML's shortcomings and

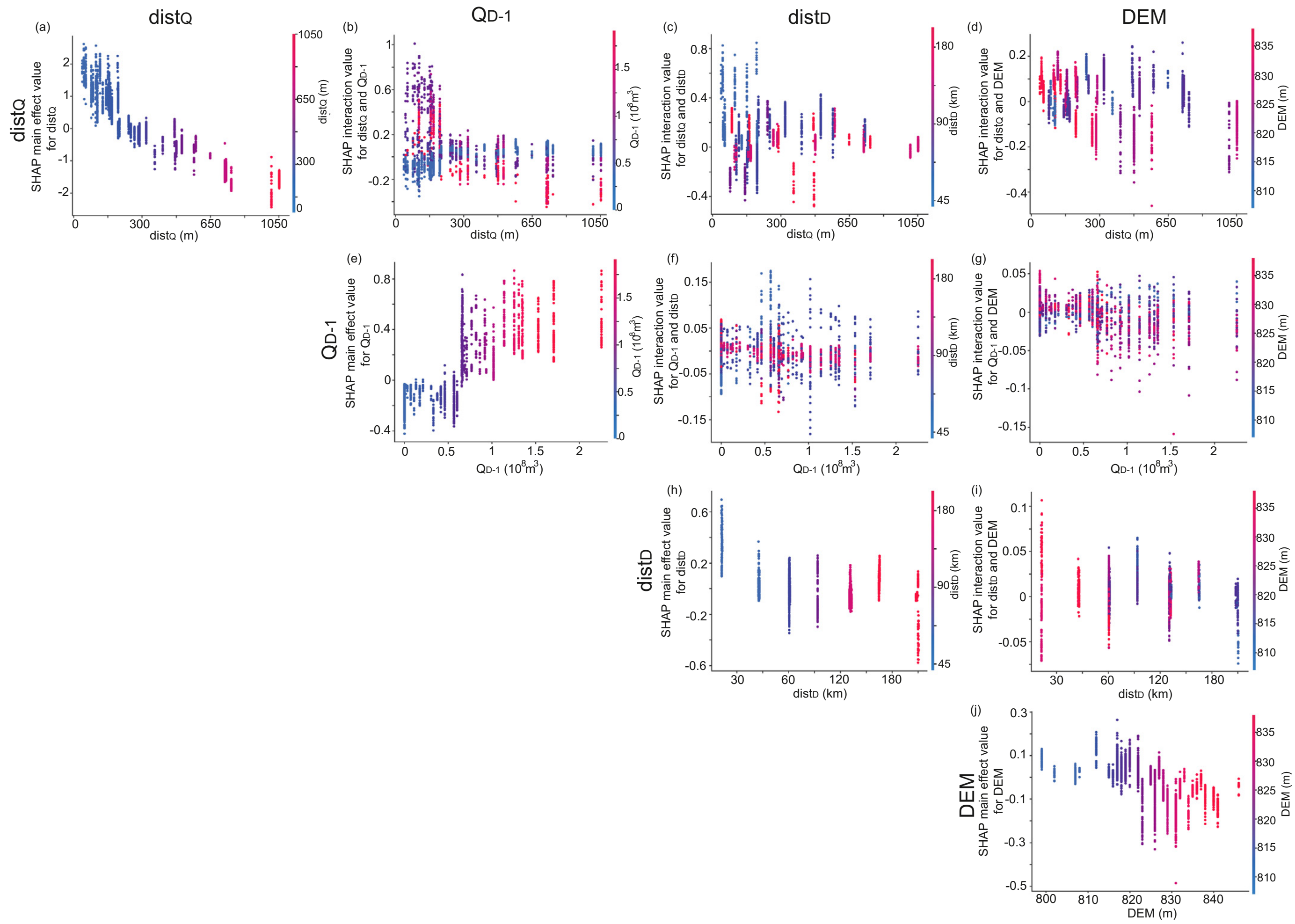

Fig. 4. SHAP interaction results of the important variables $dist_Q$, $Q_{D\text{-}1}$, $dist_D$, and DEM in the Qiwenkur river channel of the lower Tarim River basin. The vertical axis lists the interaction effect on the model's prediction for groundwater level, and the horizontal axis exhibits the variable value. The red color denotes a higher value of variables while the blue denotes a lower value. For the metric codes of the variables see Table 1.

quantitative analyses the effect of the variables on model output based on the comprehensive analysis (Wang et al., 2022). Therefore, the SHAP method is used to interpret ML algorithms and discover the influence of hydrological, environmental, and meteorological factors on groundwater dynamics in the lower Tarim River basin from global perspectives. These results help us understand how the "black box" model uses input variables to make predictions of regional groundwater levels, and also provide us a further understanding of the complex processes that give rise to the variation of groundwater.

3.3. The projection of present groundwater table

The lower reaches of Tarim River basin is known as the "green corridor" since it is located between the Taklamakan Desert and Kuruke Desert (Chen et al., 2010). However, the "green corridor" has disappeared in the 1970s as the streamflow in the lower reaches and the terminal lake Taitema Lake dried out because of dramatically increased water consumption for irrigation and domestic use in the upper-middle reaches (Tao et al., 2008; Song et al., 1999). This drying dramatically dropped the downstream groundwater level and destroyed the ecosystems, many plants decreased extensively. The Kuruk Desert and the Taklamakan Desert have tended to converge. Land desertification has intensified, and many catastrophic climatic events such as sand storms have increased. To revive the degraded ecosystems of the lower Tarim River basin, the Management Bureau of the Tarim River Basin started implementing the "Ecological Water Conveyance" project in 2000. Water was intermittently transferred from the Daxihaizi Reservoir to the downstream of the Tarim River basin through a single river channel (i.e., Qiwenkur River or Old Tarim River channel) or through double channels and finally to Taitemar Lake (Fig. 1(a) and (b)). The total volume of water conveyanced from the Daxihaizi Reservoir, Qiwenkur River channel, and Old Tarim River channel is presented in Fig. 5(a)–(c), respectively. Until 2020, a total volume of 8.445×10^9 m^3 water has already been conveyanced (Fig. 5).

However, the date, duration, and volume of each water conveyance were not fixed and were entirely controlled arbitrarily. Water conveyance duration ranged from 1 month to 10 months (Fig. 5). Although the "Ecological Water Conveyance" project considerably lifted the groundwater level to meet the water demand of natural vegetation in the lower reaches, many researchers have figured out that the date, duration, and volume of water conveyance were random and need to be optimized (Chen et al., 2010; Tao et al., 2008; Zhou et al., 2020). For example, the diversion time of the "Ecological Water Conveyance" project in the Tarim River basin is always during winter (Chen et al., 2010; Tao et al., 2008). However, the time period from August to September in each year is the seed ripening and dispersal periods of native vegetation like Populus euphratica, *Tamarix ramosissima* and Alhagi sparsifolia (Cheng et al., 2007). The water conveyance during this period will assist the spreading, germinating and natural regeneration of seeds along river channel margins (Cheng et al., 2007; Chen et al., 2010). Besides, as groundwater level is the crucial factor affecting the growth of vegetation in the lower Tarim River basin (Hao et al.,

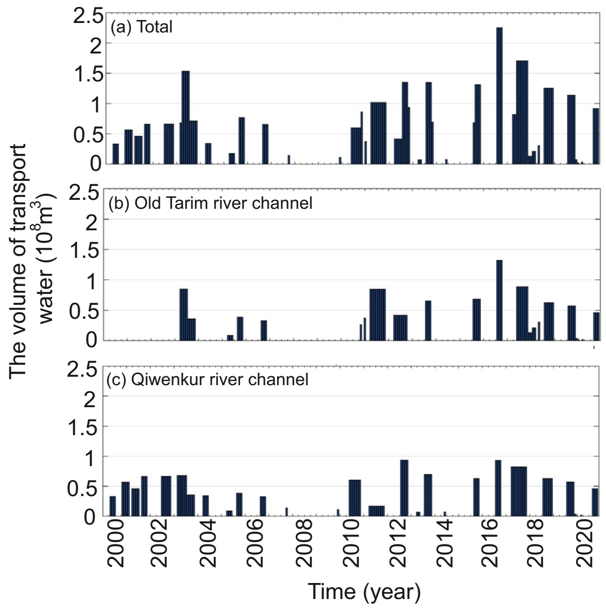

Fig. 5. The volume of water conveyanced (a) from the Daxihaizi Reservoir, (b) in the Old Tarim river channel, and (c) in the Qiwenkur river channel from January 2000 to December 2020.

2010; Zhou et al., 2020), the groundwater depth must be maintained at a minimum of 6 m in depth to meet the normal growth of natural vegetation in the lower reaches (Hao et al., 2010; Zhou et al., 2020). Therefore, it is necessary to fix the date, duration, and volume of the "Ecological Water Conveyance" project each year to timely maintain optimal groundwater depth for long-term riparian forest development since the water resource of the project is limited by upstream water inflow and agricultural water consumption, under limited water resources (Tao et al., 2008).

The RF model was selected to simulate the past and present groundwater levels because of its good accuracy among all models. The spatiotemporal distribution of the groundwater table downstream of the Tarim River from 2000 to 2020 is presented in Fig. 6. Because the "Ecological Water Conveyance" project was started in 2000 and the available groundwater level monitoring data during this time, this study focuses on the time period from 2000 to 2020. Among the several selected points, the time series plots from 2000 and 2020 (Fig. 6(a)) clearly present the variation of groundwater levels at different locations. These points include locations (Fig. 6c) at the Akdun transect (A), at the Yahepu transect (B), at the Yinsu transect (C), at the Kardayi transect (D), at the Alagan transect (E), at the Yiganbujima transect (F) with intervals of 150–300 m away from the river channel. In general, groundwater levels in all points exhibit a consistently increasing trend with water conveyance, as well as an obvious decreasing trend between 2008 and 2010 due to no water conveyance over the period (Fig. 6(a)). Compared with groundwater levels in other points, the groundwater level in point A shows an immediate increase in the first "Ecological Water Conveyance" project while groundwater levels in points E and F are found to rise after several "Ecological Water Conveyance" projects. This is intuitive since the groundwater depth in the upper section of the lower Tarim River is sensitive to the water conveyanced from the Daxihaizi Reservoir, and the response of the groundwater table gradually decreased down the riverbank (Tao et al., 2008; Chen et al., 2010).

The spatial distribution of the long-term average groundwater table and the increasing trend of groundwater table from January 2000 to December 2020 simulated by the RF model is shown in Fig. 6(b) and (c), respectively. In general, the shallower groundwater levels are mainly found in the areas near the riverbank, and the groundwater level deepens with the distance from the riverbank (Fig. 6(b)). Similarly, the SHAP results (Figs. 3 and 4) also show that the distance to the river course have the greatest impact on the variation of groundwater, and this is intuitive in most arid and semiarid regions since the groundwater close to the river course is fed more from river flow than that of the region away from the course (Tao et al., 2008). Geographically, groundwater levels in most areas exhibited an obvious increasing trend due to water conveyance between 2000 and 2020 (Fig. 6(c)). The groundwater level near the river channel, especially the Qiwenkur river channel, indicated a slightly increasing trend over 2000 to 2020 (Fig. 6(c)). Groundwater depths close to the river course were shallow during the entire study period and had relatively insignificant increases. While the long watering duration and large volumes of water conveyance played an important role in raising the groundwater depth far from the rive course (Bao et al., 2017; Chen et al., 2010). Besides, the groundwater table is not only affected by the "Ecological Water Conveyance" project, but also by altitude. The altitude gradually reduces from 846.25 m in the Daxihaizi Reservoir to 801.5 m in the lower sections downstream of the Tarim River (Liu and Chen, 2007). As illustrated in Fig. 6(b), in the lower Tarim River basin, the deeper groundwater depth generally occurs in high altitude areas (i.e., the northern and eastern regions) and gradually rises with decreasing altitude, while the highest groundwater depth distributes in the western and southern regions (Fig. 6(b)). This result is also consistent with the SHAP plot (Figs. 3 and 4) that the variable DEM shows a negative impact on the variation of groundwater while an increase in DEM also a drop in the groundwater table.

The overall changes in groundwater levels in the lower Tarim River between 2000 and 2020 simulated by the RF model are summarized in Fig. 7 (a). As expected, the groundwater levels in downstream Tarim River exhibited a similar trend with water conveyance (Figs. 5 and 7(a)). For example, groundwater levels on average increased from −6.6 m in 2000 to −5.2 m in 2003, −6.2 m in 2011 to −4.6 m in 2020 because of more frequent water conveyance, and decreased from −5.8 m in 2004 to −7.4 m in 2010 due to reduced water conveyance between 2004 and 2010 (Fig. 7 (a)). Fig. 7(b) illustrates the proportion and spatial distribution of optimum, basic, and unsuitable groundwater table for natural vegetation growth downstream of the Tarim River from 2000 to 2020. In the downstream Tarim River basin, the basic groundwater level needed by plants is 0–6 m, and the species diversity is highest at 2–4 m level (Hao et al., 2010). When the water table dropped to below 6 m, species diversity decreases greatly (Hao et al., 2010). It is clear from Fig. 7(b) that the proportion of unsuitable regions for vegetation (i.e., groundwater depth below 6 m) gradually decreased from 63.78% in 2000 to 24.68% in 2020 with the increase of water conveyance (Fig. 7(b)). This is consistent with previous studies that many herbaceous plants, such as *Apocynum venetum*, reappeared along the riverbank (Tao et al., 2008; Mamat et al., 2018), and the species composition of natural vegetation changed from 17 species before water conveyance (2000) to 46 species after conveyance. The "Ecological Water Conveyance" project in the lower Tarim River has a vital role in lifting the groundwater table, as well as creating a suitable environment for ecosystem rehabilitation. Notably, the government should convey the water at a reasonable frequency. It seems that a stable watering scheme (i.e., conveyance water annually) is more important in maintaining suitable areas for natural vegetation from a long-term perspective. For example, suitable areas for natural vegetation (i.e., groundwater levels at 0–2 m and 4–6 m) decreased from 62.65% in 2004 to 5.95% in 2010 due to reduced water conveyance between 2004 and 2006 and almost no water conveyance between 2007 and 2010 (Fig. 7(b)).

3.4. The projection of future groundwater table

To project the possible future changes of the groundwater level downstream of the Tarim River with no water conveyance during 2021–2023, the optimal model (i.e., the RF model) was employed to predict the spatiotemporal distribution of groundwater depth. The temperature and relative humidity over the study region are assumed to be under the scenario SSP245, which represents the medium pathway of future greenhouse gas emissions with an additional radiative forcing of 4.5 W m^{-2} by 2100. This scenario assumes that climate protection measures are being taken (O'Neill et al., 2016). To quantify the impacts of water diversion, the

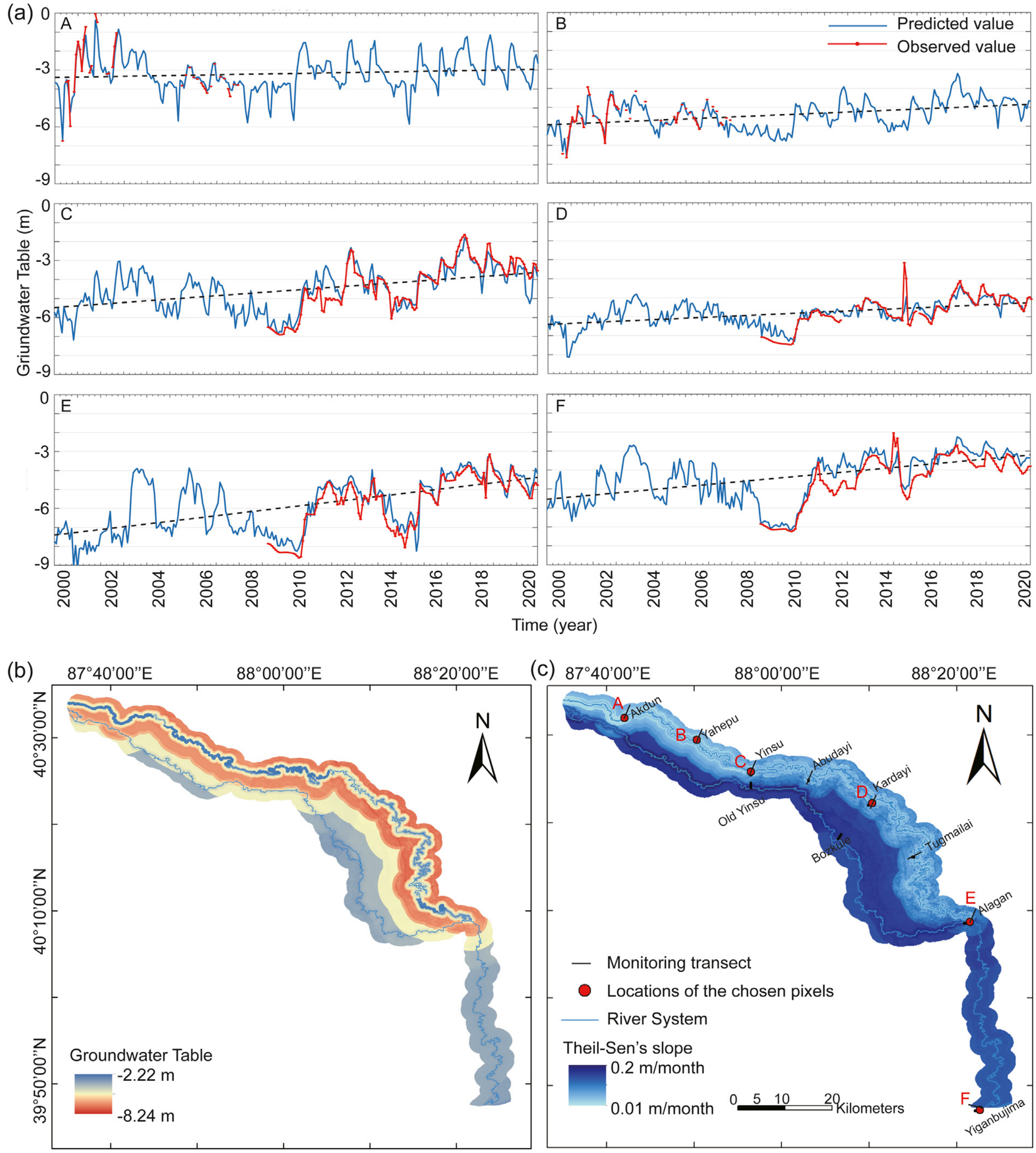

Fig. 6. (a) Time series plots of groundwater table at six different locations simulated by the RF model. (b) The long-term average groundwater table. (c) Increasing trend of groundwater table from January 2000 to December 2020, and the locations of the chosen points.

predicted results for the period 2021–2023 without water conveyance were compared with the groundwater level in the year 2020 based on the simulation of the RF model (Fig. 8(a1)). As expected, without water recharge, groundwater levels in the lower Tarim River deepens gradually as time increases. The average groundwater level decreases from −4.6 m in 2020 to −6.4 m in 2023 (Fig. 8(a2)–(a4)). Because the groundwater table deepens with the distance from the river course in the lower Tarim River (Fig. 8 (a1)–(a4)), the basic and appropriate areas for desert riparian vegetation (Fig. 8(b1)–(b4)) are mainly found near the riverbank, and the area decreases with the distance from the riverbank (Fig. 8(b1)–(b4)). Notably, without water conveyance, the unsuitable region for plant growth increased from 25% in 2020 to 61% in 2023 under the SSP245 scenario, and the optimal region for plant growth (i.e., groundwater levels at 2–4 m) decreased from 37% in 2020 to 2% in 2023 (Fig. 8(b4)). To guarantee the stability of groundwater-dependent ecosystems in the lower Tarim River basin, it is necessary to convey the water continuously at annual time scales (Liu et al., 2022).

Climate change is intensifying the conflict between water supply and demand as droughts increase in many regions of the world (Yuan et al., 2019). There are previous studies focusing on the impacts of climate change on water resources in the lower Tarim River basin (Li et al., 2021; Shen et al., 2018; Tao et al., 2011). In the lower reaches of Tarim River, the “Ecological Water Conveyance” project is the only water source for groundwater (Tao et al., 2008), and water supplies in the project are controlled by the streamflow coming from the headstreams to the upper-middle reaches. On the one hand, although the stream from the headstreams of Tarim

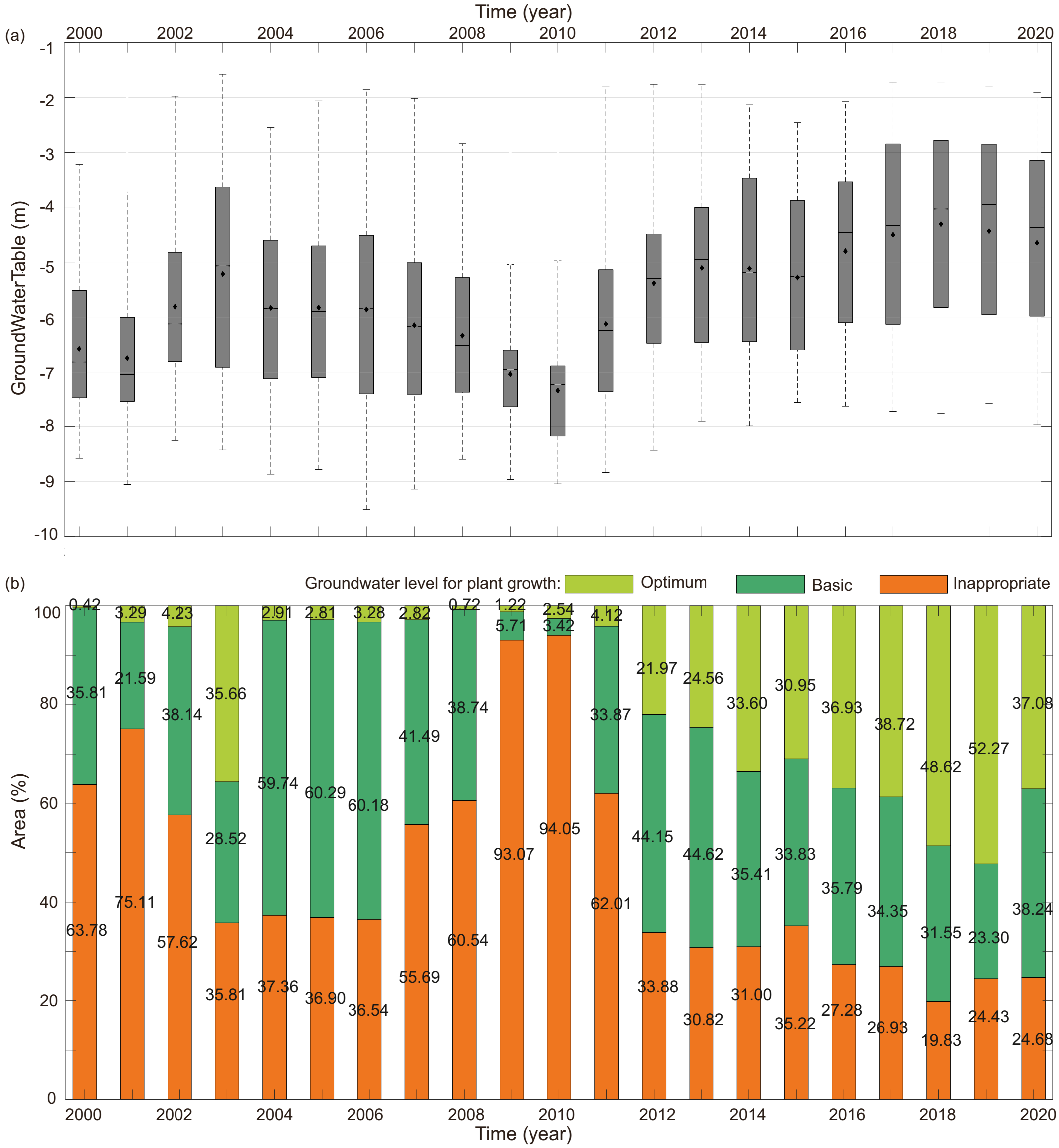

Fig. 7. (a) The boxplot of groundwater table in the study area between 2000 and 2020 simulated by the RF model. (b) Area of the optimal, basic, and unsuitable groundwater level for plants in the study area between 2000 and 2020.

River is susceptible to climate change and show increasing trends because increases in precipitation and temperature directly increase streamflow and snowmelt runoff in headstreams (Shen et al., 2018; Tao et al., 2011), anthropogenic activities such as domestic use and irrigation strongly reduce the main stream of Tarim River (Tao et al., 2011). On the other hand, global climate change may lead to an earlier start and a later end of the growing season (Li et al., 2021), which would cause more drought, and warming would also intensify potential evapotranspiration (Su et al., 2018). These all influence the variation of the groundwater table in the lower Tarim River. Further research will be implemented in future work to quantitatively assess the impact of climate change on the lower Tarim River.

Groundwater level prediction is critical for sustainable management of water resources, particularly for drylands where there is a strong need to manage groundwater resources in a dynamically effective way so that they should be available for human and ecosystem needs (Tapoglou et al., 2014; Zuo et al., 2021). The lower Tarim River basin is an extremely arid region with annual precipitation approximately of 17–35 mm, groundwater dynamics mainly dominated by the “Ecological Water Conveyance” project (Tao et al., 2008). And it is representative in many arid regions where groundwater is mainly fed by intermittent streams like the “Ecological Water Conveyance” project, such as the Heihe River basin, and the Shiyang River basin in Northwest China, and the Aral Sea basin in Central Asia (Shen et al., 2017; Shumilova et al., 2018). An accurate and reliable regional-scale groundwater estimation is necessary in these regions as groundwater depth is the crucial environmental factors affecting the growth of desert vegetation (Hao et al., 2010). This intermittent recharge mode increases the difficulty of regional groundwater simulation. Moreover, groundwater monitoring data in arid regions are usually spatiotemporal discontinuous because of limitations like labor and funding (Ruybal et al., 2019). For example, groundwater level observations in the lower Tarim River basin have many spatiotemporal gaps in the record, and less

Fig. 8. The groundwater table in the downstream Tarim River (a1) estimated using the RF model from January 2020 to December 2020, and (a2–a4) predicted with no water conveyance during 2021 and 2023 under future climate scenarios SSP245. The area and spatial distribution of groundwater table for desert riparian vegetation downstream of Tarim River (b1) estimated using the RF model from January 2020 to December 2020, and (b2–b4) predicted in case of no water diversion during 2021 and 2023 under future climate scenarios SSP245.

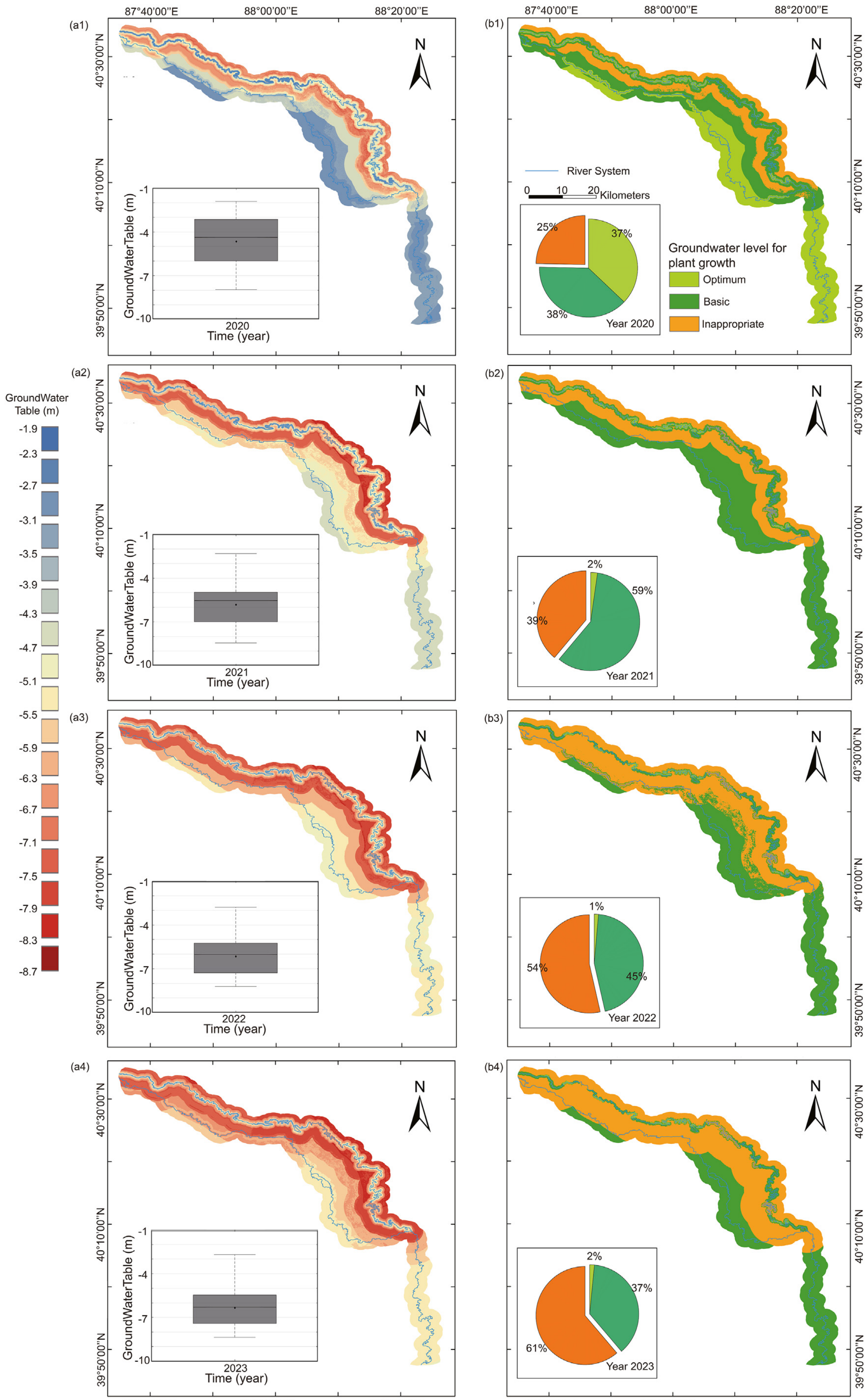
(a1)
(a2)
(a3)
(a4)
(b1)
(b2)
(b3)
(b4)
87°40'00"E
88°00'00"E
88°20'00"E
40°30'00"N
40°10'00"N
39°50'00"N
N
GroundWater Table (m)
-1.9
-2.3
-2.7
-3.1
-3.5
-3.9
-4.3
-4.7
-5.1
-5.5
-5.9
-6.3
-6.7
-7.1
-7.5
-7.9
-8.3
-8.7
GroundWaterTable (m)
-1
-4
-7
-10
2020
2021
2022
2023
Time (year)
River System
0 10 20 Kilometers
Groundwater level for plant growth
Optimum
Basic
Inappropriate
25%
37%
38%
Year 2020
2%
59%
39%
Year 2021
1%
54%
45%
Year 2022
2%
37%
61%
Year 2023

than 17% of the well records included a continuous observation of the months between 2009 and 2020 (Fig. 1(d)). Such case also increases the difficulty of the extensive application of geostatistical methods in regional groundwater simulation in arid regions.

Many studies on the variation of groundwater depth in the lower Tarim River were focused on the changes of groundwater depth in groundwater monitoring wells (Chen et al., 2010; Tao et al., 2008; Hao and Li, 2014). Because traditional physical-based models require explicit quantification of physical properties (Szidarovszky et al., 2007), given the inadequate information and uncertain parameters (Liu et al., 2021), the widespread application of physical-based models in the prediction of groundwater depth in the lower Tarim River was limited. Most physical-based modelings of groundwater were merely developed in some sections of the downstream Tarim River (Liu et al., 2019, 2021; Ye et al., 2009). The ML modeling developed in this study is able to utilize such spatiotemporally inconsistent monitoring data (Fig. 1d) to generate the spatiotemporal variation of the groundwater system in arid regions where exist stream or intermittent flow. Because unlike physical-based models which require explicit and accurate characterization of the physics, these data-driven models can find the complicated nonlinear connections within the sample data without a prior assumption that specific relationships exist the inputs and outputs (LeCun et al., 2015; Yin et al., 2021). The model developed here with easily available input data such as temperature, relative humidity, distance to the river channel, and volume of the stream or conveyanced water, are capable of extracting the relation between inputs and groundwater levels.

4. Conclusions

In this study, an evaluation and comparison of the accuracy of SVM, GRNN, DT, RF, CNN, LSTM, and GRU models in predicting the spatiotemporal distribution of groundwater levels in the arid lower Tarim River basin have been conducted. RF is superior to other models in one-step-ahead predictions of groundwater depth in the space-time domain. RF model developed here with easily available input data, such as temperature, relative humidity, flow volume, and geospatial information like DEM and the distance to the riverbank, can fully utilize spatiotemporally inconsistent groundwater monitoring data to modeling the spatiotemporal variation of groundwater in arid regions where groundwater recharge is mainly dominated by intermittent flow like water conveyance projects. Using the SHAP method to interpret the ML models, which are plagued by their characteristic of "black box", can quantitatively analyze the magnitude and direction of the impact of meteorological, hydrological, and environmental factors on the regional groundwater table. According to the SHAP analysis, the flow volume and the distance to the river channel and reservoir have critical impacts on groundwater changes in the lower Tarim River basin. Within 300 m distance, conveyanced more than 0.7×10^8 m^3 water can dramatically lift the groundwater level in the lower Tarim River basin. While far from the riverbank, the effects on groundwater depth decreased gradually further away from the river course. Because this study major focused on the prediction of groundwater in the lower Tarim River using SHAP for model interpretation, it has more explanatory power than previous studies using data-driven models (Xu et al., 2008, 2013; Zuo et al., 2021).

From the simulated results, "Ecological Water Conveyance" projects played a very important role in lifting the groundwater table in the lower Tarim River: the groundwater depth on average increased from −6.6 m in 2000 to −4.6 m in 2020, and the appropriate areas for plant growth increased from 36.22% in 2000 to 75.32% in 2020. Within the next three years (2021–2023), the average groundwater level may be reduced to −6.4 m, and the suitable areas for natural vegetation are limited to 39% of the geographic space if no stream or intermittent flow is recharged. Riparian vegetation is an integral component of ecosystems and is essential for maintaining many critical ecosystem services. Maintaining an appropriate groundwater level is necessary to sustain the stability and structure of vegetation communities since the survival of riparian vegetation in the arid region depends almost entirely on groundwater. Continuous annual water conveyance is necessary for long-term riparian forest development. The findings of this study have demonstrated the present and future variations of groundwater level from a quantitative perspective, which have important scientific implications for informed decision making regarding sustainable water resources management in arid regions where groundwater recharge is mainly dominated by streams or intermittent flow like water conveyance projects. To obtain higher precision of regional groundwater level prediction, further research is needed. For example, because past groundwater level data is often limited for most regions in a real-world scenario and cannot be used as model input to improve the model performance, further research could also be extended to include the Gravity Recovery and Climate Experiment (GRACE) satellites data, which provides the changes in total water storage at all depths, among its input variables to improve the performance of groundwater level predictions. Further research should attempt to integrate the process-based model to add the physical mechanism in ML algorithms and thereby make it more understandable. SHAP method shows the positive and negative relationship between groundwater depth and meteorological, hydrological, and environmental variables, and helps us to understand the processes that give rise to the variation of the groundwater system in arid regions and is useful for interpreting ML models in water science research.

CRediT authorship contribution statement

Gui Dongwei: Conceptualization, Methodology, Writing - Reviewing and Editing. **Liu Qi**: Data curation, Software, Writing - Original draft preparation. **Zhang Lei**; **Wei Guanghui**; **Dai Heng**; **Bill X. Hu**: Visualization, Investigation. **Niu Jie**: Supervision, Writing - Reviewing and Editing.

Declaration of competing interest

The authors declare that they have no known competing financial interests or personal relationships that could have appeared to influence the work reported in this paper.

Acknowledgments

This work is supported by the National Natural Science Foundation of China (41972244, 42171042). The authors declare no conflict of interest.

References

Allen, R.G., Pereira, L.S., Raes, D., Smith, M., 1998. Crop evapotranspiration—guidelines for computing crop water requirements. FAO Irrigation and Drainage Paper 56. Technical Report. Rome. 56, pp. 15–64.

Bao, A., Huang, Y., Ma, Y., Guo, H., Wang, Y., 2017. Assessing the effect of EWDP on vegetation restoration by remote sensing in the lower reaches of Tarim River. Ecol. Indic. 74, 261–275. https://doi.org/10.1016/j.ecolind.2016.11.007.

Basu, B., Morrissey, P., Gill, L.W., 2022. Application of nonlinear time series and machine learning algorithms for forecasting groundwater flooding in a lowland karst area. Water Resources Research 58, e2021WR029576. https://doi.org/10.1029/2021WR029576.

Breiman, L., 2001. Random forests. Mach. Learn. 45, 5–32. https://doi.org/10.1023/A:1010933404324.

Breiman, L., Friedman, J.H., Olshen, R.A., Stone, C.J., 1984. Classification and Regression Trees. Chapman & Hall, Boca Raton, FL, USA.

Chen, Y., Chen, Y., Xu, C., Ye, Z., Li, Z., Zhu, C., Ma, X., 2010. Effects of ecological water conveyance on groundwater dynamics and riparian vegetation in the lower reaches of Tarim RiverChina. Hydrol. Process. 24, 170–177. https://doi.org/10.1002/hyp.7429.

Chen, C., He, W., Zhou, H., Xue, Y., Zhu, M., 2020. A comparative study among machine learning and numerical models for simulating groundwater dynamics in the Heihe River basin, northwestern China. Sci. Rep. 10, 904.

Chen, Z., Liu, Y., Sun, H., 2021. Physics-informed learning of governing equations from scarce data. NatureCommunications 12.

Cheng, K.W., Zang, R.G., Zhou, X.F., Zhang, W.Y., Bai, Z.Q., 2007. Influence of floods on natural riparian forests along the Ergis River, West China. Front. For. China 2 (1), 66–71. https://doi.org/10.1007/s11461-007-0010-7.

Chung, J., Gulcehre, C., Cho, K., Bengio, Y., 2014. Empirical evaluation of gated recurrent neural networks on sequence modeling. NIPS 2014 Workshop on Deep Learning preprint arXiv:1412.3555.

Condon, L.E., Maxwell, R.M., 2015. Evaluating the relationship between topography and groundwater using outputs from a continental-scale integrated hydrology model. Water Resour. Res. 51, 6602–6621. https://doi.org/10.1002/2014WR016774.

Dilip, K., Rajib, K.B., 2021. GRNN model for prediction of groundwater fluctuation in the state of Uttarakhand of India using GRACE data under limited bore well data. J. Hydroinf. 23 (3), 567–588. https://doi.org/10.2166/hydro.2021.108.

Fang, K., Shen, C., 2020. Near-real-time forecast of satellite-based soil moisture using long short-term memory with an adaptive data integration kernel. J. Hydrometeorol. 21 (3), 399–413. https://journals.ametsoc.org/view/journals/hydr/21/3/jhm-d-19-0169.1.xml.

Gaur, M., Squires, V., 2018. Geographic Extent and Characteristics of the World's Arid Zones and Their Peoples. https://doi.org/10.1007/978-3-319-56681-8_1.

Gaye, B., Zhang, D., Wulamu, A., 2021. Improvement of support vector machine algorithm in big data background. Math. Probl. Eng. 2021, 5594899. https://doi.org/10.1155/2021/5594899.

Ghayoumian, J., Mohseni, S.M., Feiznia, S., Nouri, B., Malekian, A., 2007. Application of GIS techniques to determine areas most suitable for artificial groundwater recharge in a coastal aquifer in southern Iran. J. Asian Earth Sci. 30, 364–374. https://doi.org/10.1016/j.jseaes.2006.11.002.

Govindaraju, R.S., 2000. Artificial neural networks in hydrology. II: hydrologic applications. J. Hydrol. Eng. 5 (2), 124–137.

Gupta, H.V., Sorooshian, S., Yapo, P.O., 1999. Status of automatic calibration for hydrologic models: comparison with multilevel expert calibration. J. Hydrol. Eng. 4 (2), 135–143.

Hao, X., Li, W., 2014. Impacts of ecological water conveyance on groundwater dynamics and vegetation recovery in the lower reaches of the Tarim River in Northwest China. Environ. Monit. Assess. 186 (11), 7605–7616. https://doi.org/10.1007/s10661-014-3952-x.

Hao, X., Li, W., Huang, X., Zhu, C., Ma, J., 2010. Assessment of the groundwater threshold of desert riparian forest vegetation along the middle and lower reaches of the Tarim RiverChina. Hydrol. Process. 24, 178–186. https://doi.org/10.1002/hyp.7432.

Hashemi, H., Berndtsson, R., Kompani, Z.M., Persson, M., 2013. Natural vs. artificial groundwater recharge, quantification through inverse modeling. Hydrol. Earth Syst. Sci. 17, 637–650. https://doi.org/10.5194/hess-17-637-2013 2013.

Hengl, T., 2007. A practical guide to geostatistical mapping of environmental variables. Geoderma 140 (4), 417–427.

Huang, T., Pang, Z., 2010. Changes in groundwater induced by water diversion in the lower Tarim River, Xinjiang Uygur, NW China: evidence from environmental isotopes and water chemistry. J. Hydrol. 387, 188–201. https://doi.org/10.1016/j.jhydrol.2010.04.007.

Jeihouni, E., Eslamian, S., Mohammadi, M., Zareian, M.J., 2019. Simulation of groundwater level fluctuations in response to main climate parameters using a wavelet-ANN hybrid technique for the Shabestar plainIran. Environmental Earth Science 78, 293.

Koch, J., Berger, H., Henriksen, H.J., Sonnenborg, T.O., 2019. Modelling of the shallow water table at high spatial resolution using random forests. Hydrol. Earth Syst. Sci. 23, 4603–4619. https://doi.org/10.5194/hess-23-4603-2019.

LeCun, Y., Bengio, Y., Hinton, G., 2015. Deep learning. Nature 521, 436–444. https://doi.org/10.1038/nature14539.

Li, X., Ding, Q., Sun, J.Q., 2018. Remaining useful life estimation in prognostics using deep convolution neural networks. Reliab. Eng. Syst. Saf. 172, 1–11.

Li, H., Feng, J., Bai, L., Zhang, J., 2021. Populus euphratica phenology and its response to climate change in the upper Tarim River basin, NW China. Forests 12, 1315. https://doi.org/10.3390/f12101315.

Ling, H., Zhang, P., Xu, H., Zhang, G., 2016. Determining the ecological water allocation in a hyper-arid catchment with increasing competition for water resources. Glob. Planet. Chang. 145, 143–152. https://doi.org/10.1016/j.gloplacha.2016.08.012.

Liu, Y., Chen, Y., 2007. Saving the "Green Corridor": recharging groundwater to restore riparian Forest along the lower Tarim River, China. Ecological Restoration. 25 (2), 112–117. http://www.jstor.org/stable/43443055.

Liu, Q., Hanati, G., Danierhan, S., Zhang, Y., Zhang, Z., 2019. Simulation of groundwater level in ephemeral streams with an improved groundwater hydraulics model. Groundwater 57, 969–979. https://doi.org/10.1111/gwat.12914.

Liu, Q., Hanati, G., Danierhan, S., 2021. Modeling of multiyear water-table fluctuations in response to intermittent artificial recharge. Hydrogeol. J. 29, 2397–2410. https://doi.org/10.1007/s10040-021-02388-y.

Liu, Q., Dai, H., Gui, D.W., Hu, B., Ye, M., Wei, G., Qin, J., Zhang, J., 2022. Evaluation and optimization of the water diversion system of ecohydrological restoration megaproject of Tarim River, China, through wavelet analysis and a neural network. J. Hydrol. 608, 127586. https://doi.org/10.1016/j.jhydrol.2022.127586.

Long, D., Yang, W., Scanlon, B.R., 2020. South-to-north water diversion stabilizing Beijing's groundwater levels. Nat. Commun. 11, 3665. https://doi.org/10.1038/s41467-020-17428-6.

Lundberg, S.M., Lee, S.I., 2017. A unified approach to interpreting model predictions. Adv. Neural Inf. Process. Syst. 30, 4766–4775.

Mamat, Z., Halik, Ü., Keyimu, M., Keram, A., Nurmamat, K., 2018. Variation of the floodplain forest ecosystem service value in the lower reaches of Tarim River, China. Land Degradation & Development. 29, 47–57. https://doi.org/10.1002/ldr.2835.

Messager, M.L., Lehner, B., Cockburn, C., Lamouroux, N., Pella, H., Snelder, T., Tockner, K., Trautmann, T., Watt, C., Datry, T., 2021. Global prevalence of non-perennial rivers and streams. Nature 594 (7863), 391–397. https://doi.org/10.1038/s41586-021-03565-5.

Moghaddam, H.K., Moghaddam, H.K., Kivi, Z.R., Bahreinimotlagh, M., Alizadeh, M.J., 2019. Developing comparative mathematic models, BN and ANN for forecasting of groundwater levels. Groundwater Sustainable 9, 100237. https://doi.org/10.1016/j.gsd.2019.100237.

Montano, M.J.J., Palmer, P.A., Munoz, G.P., 2011. Artificial neural networks applied to forecasting time series. Psicothema. 23 (2), 322–329.

Nearing, G.S., Kratzert, F., Sampson, A.K., Pelissier, C.S., Klotz, D., Frame, J.M., Prieto, C., Gupta, H.V., 2020. What role does hydrological science play in the age of machine learning? Water Resour. Res. https://doi.org/10.1029/2020WR028091.

Nguyen, H., Babel, M., Weesakul, S., Tripathi, N., 2009. An artificial neural network model for rainfall forecasting in Bangkok, Thailand. Hydrology and Earth System Sciences. 13. https://doi.org/10.5194/hess-13-1413-2009.

O'Neill, B.C., Tebaldi, C., van Vuuren, D.P., Eyring, V., Friedlingstein, P., Hurtt, G., Knutti, R., Kriegler, E., Lamarque, J.F., Lowe, J., Meehl, G.A., Moss, R., Riahi, K., Sanderson, B.M., 2016. The scenario model intercomparison project (ScenarioMIP) for CMIP6. Geosci. Model Dev. 9, 3461–3482. https://doi.org/10.5194/gmd-9-3461-2016.

Raissi, M., Perdikaris, P., Karniadakis, G.E., 2017. Physics informed deep learning (part I): data-driven solutions of nonlinear partial differential equations. ArXiv abs/1711.10561.

Raissi, M., Perdikaris, P., Karniadakis, G.E., 2018. Physics-informed Neural Networks: A Deep Learning Framework for Solving Forward and Inverse Problems Involving Nonlinear Partial Differential Equations. United States. https://doi.org/10.1016/j.jcp.2018.10.045.

Rajaee, T., Ebrahimi, H., Nourani, V., 2019. A review of the artificial intelligence methods in groundwater level modeling. J. Hydrol. 572. https://doi.org/10.1016/j.jhydrol.2018.12.037.

Russo, T., Lall, U., 2017. Depletion and response of deep groundwater to climate-induced pumping variability. Nat. Geosci. 10, 105–108. https://doi.org/10.1038/ngeo2883.

Ruybal, C.J., Hogue, T.S., McCray, J.E., 2019. Evaluation of groundwater levels in the Arapahoe aquifer using spatiotemporal regression kriging. Water Resour. Res. 55, 2820–2837. https://doi.org/10.1029/2018WR023437.

Sahoo, M., Das, T., Kumari, K., Dhar, A., 2017. Space–time forecasting of groundwater level using a hybrid soft computing model. Hydrol. Sci. J. 62, 561–574. https://doi.org/10.1080/02626667.2016.1252986.

Sen, P.K., 1968. Estimates of the regression coefficient based on Kendall's tau. J. Am. Stat. Assoc. 63 (324), 1379–1389. https://doi.org/10.1080/01621459.1968.10480934.

Shen, Q., Gao, G.Y., Lu, Y.H., Wang, S., Jiang, X.H., Fu, B.J., 2017. River flow is critical for vegetation dynamics: lessons from multi-scale analysis in a hyper-arid endorheic basin. Sci. Total Environ. 290–298. https://doi.org/10.1016/j.scitotenv.2017.06.087.

Shen, Y.J., Shen, Y., Fink, M., Kralisch, S., Chen, Y., Brenning, A., 2018. Trends and variability in streamflow and snowmelt runoff timing in the southern Tianshan Mountains. J. Hydrol. 557, 173–181. https://doi.org/10.1016/j.jhydrol.2017.12.035.

Sherif, M., Kacimov, A., Javadi, A., Ebraheem, A.Z., 2012. Modeling groundwater flow and seawater intrusion in the coastal aquifer of Wadi ham, UAE. Water Resour Manag. 26, 751–774.

Shumilova, O., Tockner, K., Thieme, M., Koska, A., Zarfl, C., 2018. Global water transfer megaprojects: a potential solution for the water-food-energy nexus? Front. Environ. Sci 6, 150. https://doi.org/10.3389/fenvs.2018.00150.

Singh, A., 2014. Groundwater resources management through the applications of simulation modeling: a review. Sci. Total Environ. 499, 414–423. https://doi.org/10.1016/j.scitotenv.2014.05.048.

Smola, A., 1998. Learning With Kernels. Ph.D. Thesis. Technischen Universitat Berlin, Berlin, Germany.

Song, Y.D., Fan, Z.L., Lei, Z.D., 1999. Research on Water Resources and Ecology of Tarim River, China (in Chinese). Xinjiang People's Press, Urumqi, pp. 398–418.

Specht, D.F., 1991. A general regression neural network. IEEE Trans. Neural Netw. 2 (6), 568–576.

Su, B., Huang, J., Fischer, T., Wang, Y., Kundzewicz, Z.W., Zhai, J., Sun, H., Wang, A., Zeng, X., Wang, G., Tao, H., Gemmer, M., Li, X., Jiang, T., 2018. Drought losses in China might double between the 1.5 °C and 2.0 °C warming. Proc. Natl. Acad. Sci. U. S. A. https://doi.org/10.1073/pnas.1802129115.

Szidarovszky, F., Coppola, E., Long, J., Hall, A., Poulton, M., 2007. A hybrid artificial neural network-numerical model for groundwater problems. Groundwater 45 (5), 590–600.

Tao, H., Gemmer, M., Song, Y., Jiang, T., 2008. Ecohydrological responses on water diversion in the lower reaches of the Tarim River, China. Water Resources Research. 44, W08422. https://doi.org/10.1029/2007WR006186.

Tao, H., Gemmer, M., Bai, Y., Su, B., Mao, W., 2011. Trends of streamflow in the Tarim River basin during the past 50 years: human impact or climate change? J. Hydrol. 400 (1), 1–9. https://doi.org/10.1016/j.jhydrol.2011.01.016.

Tapoglou, E., Karatzas, G.P., Trichakis, I.C., Varouchakis, E.A., 2014. A spatio-temporal hybrid neural network-Kriging model for groundwater level simulation. J. Hydrol. 519, 3193–3203. https://doi.org/10.1016/j.jhydrol.2014.10.040.

Tsai, W.P., Feng, D., Pan, M., Beck, H., Lawson, K., Yang, Y., Liu, J., Shen, C., 2021. From calibration to parameter learning: harnessing the scaling effects of big data in geoscientific modeling. Nat. Commun. 12, 5988. https://doi.org/10.1038/s41467-021-26107-z.

Varouchakis, E.A., Hristopulos, D.T., 2013. Comparison of stochastic and deterministic methods for mapping groundwater level spatial variability in sparsely monitored basins. Environ. Monit. Assess. 185 (1), 1–19.

Wang, J., Song, C., Reager, J.T., 2018. Recent global decline in endorheic basin water storages. Nat. Geosci. 11, 926–932. https://doi.org/10.1038/s41561-018-0265-7.

Wang, T.H., Yang, D.W., Yang, Y.T., Piao, S.L., Li, X., Cheng, G.D., Fu, B.J., 2020. Permafrost thawing puts the frozen carbon at risk over the Tibetan plateau. Sci. Adv. 6 (19), 1–8. https://doi.org/10.1126/sciadv.aaz3513.

Wang, R., Kim, J.H., Li, M.H., 2021. Predicting stream water quality under different urban development pattern scenarios with an interpretable machine learning approach. Sci. Total Environ. 761, 144057. https://doi.org/10.1016/j.scitotenv.2020.144057.

Wang, S., Peng, H., Liang, S., 2022. Prediction of estuarine water quality using interpretable machine learning approach. J. Hydrol. 605, 127320. https://doi.org/10.1016/j.jhydrol.2021.127320.

Wunsch, A., Liesch, T.J., Broda, S., 2018. Forecasting groundwater levels using nonlinear autoregressive networks with exogenous input (NARX). J. Hydrol. 567, 743–758. https://doi.org/10.1016/j.jhydrol.2018.01.045.

Wunsch, A., Liesch, T., Broda, S., 2021. Groundwater level forecasting with artificial neural networks: a comparison of long short-term memory (LSTM), convolutional neural networks (CNNs), and non-linear autoregressive networks with exogenous input (NARX). Hydrol. Earth Syst. Sci. 25, 1671–1687. https://doi.org/10.5194/hess-25-1671-2021.

Xu, J.H., Chen, Y.N., Li, W.H., 2008. Using GM (1, 1) models to predict groundwater level in the lower reaches of Tarim River: a demonstration at Yingsu section. 2008 IEEE Conference on Fuzzy Systems and Knowledge Discovery. 3, pp. 668–672.

Xu, J., Chen, Y., Li, W., Zhang, Y., 2013. The dynamic of groundwater level in the lower reaches of Tarim River affected by transported water from upper reaches. Water 7, 66–79.

Yang, P., Xia, J., Zhang, Y.Y., Zhan, C.S., Sun, S.X., 2019. How is the risk of hydrological drought in the Tarim River basin, Northwest China? Sci. Total Environ. 693, 133555. https://doi.org/10.1016/j.scitotenv.2019.07.361.

Yang, C., Chen, M., Yuan, Q., 2021. The application of XGBoost and SHAP to examining the factors in freight truck-related crashes: an exploratory analysis. Accid. Anal. Prev. 158, 106153. https://doi.org/10.1016/j.aap.2021.106153.

Ye, Z.X., Chen, Y.N., Li, W.H., Yan, Y., Wan, J.H., 2009. Groundwater fluctuations induced by ecological water conveyance in the lower Tarim River, Xinjiang, China. Journal of Arid Environments 73 (8), 726–732.

Yin, W.J., Fan, Z.W., Tangdamrongsub, N., Hu, L.T., Zhang, M.L., 2021. Comparison of physical and data-driven models to forecast groundwater level changes with the inclusion of GRACE – a case study over the state of Victoria, Australia. Journal of Hydrology 602, 126735. https://doi.org/10.1016/j.jhydrol.2021.126735.

Yoon, H., Jun, S.C., Hyun, Y., Bae, G.O., Lee, K.K., 2011. A comparative study of artificial neural networks and support vector machines for predicting groundwater levels in a coastal aquifer. J. Hydrol. 396 (1–2), 128–138.

Yuan, R.Q., Chang, L.L., Gupta, H., Niu, G.Y., 2019. Climatic forcing for recent significant terrestrial drying and wetting. Adv. Water Resour. 133, 103425. https://doi.org/10.1016/j.advwatres.2019.103425.

Zeydalinejad, N., 2022. Artificial neural networks Vis-à-Vis MODFLOW in the simulation of groundwater: a review. Model. Earth Syst. Environ. 1–22. https://doi.org/10.1007/s40808-022-01365-y.

Zhou, H., Chen, Y., Zhu, C., Li, Z., Fang, G., Li, Y., Fu, A., 2020. Climate change may accelerate the decline of desert riparian forest in the lower Tarim River, northwestern China: evidence from tree-rings of Populus euphratica. Ecol. Indic. 111, 105997.

Zuo, J.P., Xu, J.H., Chen, Y.N., Li, W., 2021. Downscaling simulation of groundwater storage in the Tarim River basin in Northwest China based on GRACE data. Phys. Chem. Earth 123, 103–142.